JOINT TRANSPORTATION
RESEARCH PROGRAM
INDIANA DEPARTMENT OF TRANSPORTATION
AND PURDUE UNIVERSITY

Assessment of Temperature Correction Factors for Falling Weight Deflectometer Deflections

Pablo Orosa Iglesias, Jin Li, Bongsuk Park,
Seonghwan Cho, and John E. Haddock

SPR-4717 • Report Number: FHWA/IN/JTRP-2026/01 • DOI: 10.5703/1288284318609

RECOMMENDED CITATION

Orosa Iglesias, P., Li, J., Park, B., Cho, S., & Haddock, J. E. (2026). *Assessment of temperature correction factors for falling weight deflectometer deflections* (Joint Transportation Research Program Publication No. FHWA/IN/JTRP-2026/01). West Lafayette, IN: Purdue University. https://doi.org/10.5703/1288284318609

AUTHORS

Pablo Orosa Iglesias, PhD
Lyles School of Civil and Construction Engineering
Purdue University

Jin Li, PhD
Lyles School of Civil and Construction Engineering
Purdue University

Bongsuk Park, PhD
Department of Civil Engineering
Montana Technological University

Seonghwan Cho, PhD
Division of Research and Development
Indiana Department of Transportation
(765) 429-9219
scho@indot.in.gov
Corresponding Author

John E. Haddock, PhD
Lyles School of Civil and Construction Engineering
Purdue University

JOINT TRANSPORTATION RESEARCH PROGRAM

The Joint Transportation Research Program serves as a vehicle for INDOT collaboration with higher education institutions and industry in Indiana to facilitate innovation that results in continuous improvement in the planning, design, construction, operation, management and economic efficiency of the Indiana transportation infrastructure. Learn more at engineering.purdue.edu/JTRP.

Published reports of the Joint Transportation Research Program are available at docs.lib.purdue.edu/jtrp/.

NOTICE

TECHNICAL REPORT DOCUMENTATION PAGE

1. Report No. FHWA/IN/JTRP-2026/01	2. Government Accession No.	3. Recipient's Catalog No.
4. Title and Subtitle Assessment of temperature correction factors for falling weight deflectometer deflections		**5. Report Date** January 16, 2026 **6. Performing Organization Code**
7. Author(s) Pablo Orosa Iglesias, PhD (https://orcid.org/0000-0003-2198-1955) Jin Li, PhD (https://orcid.org/0000-0002-3120-5573) Bongsuk Park, PhD (https://orcid.org/0000-0003-4606-4408) Seonghwan Cho, PhD (https://orcid.org/0000-0001-7938-2694) John E. Haddock, PhD (https://orcid.org/0000-0002-8030-317X)		**8. Performing Organization Report No.** FHWA/IN/JTRP-2026/01
9. Performing Organization Name and Address Joint Transportation Research Program Hall for Discovery and Learning Research (DLR), Suite 204 207 S. Martin Jischke Drive West Lafayette, IN 47907		**10. Work Unit No.** **11. Contract or Grant No.** SPR-4717
12. Sponsoring Agency Name and Address Indiana Department of Transportation (SPR) State Office Building 100 North Senate Avenue Indianapolis, IN 46204		**13. Type of Report and Period Covered** Final Report **14. Sponsoring Agency Code**

15. Supplementary Notes

Conducted in cooperation with the U.S. Department of Transportation, Federal Highway Administration.

16. Abstract

This study presents the development of an improved temperature correction methodology for falling weight deflectometer (FWD) deflections in full-depth asphalt pavements. The objective was to address the limitations of existing correction methods by integrating viscoelastic pavement behavior, structural properties, and realistic thermal gradients. Field temperature data from instrumented sites in Indiana were used to train a machine learning model capable of predicting pavement temperature profiles in flexible pavements. These predictions informed a series of finite element simulations that captured pavement responses to FWD loading under a range of thermal and structural conditions. Temperature correction factors were then derived and modeled using a unified sigmoidal function, whose parameters depend solely on asphalt thickness, subgrade stiffness, and effective pavement temperature. For full-depth asphalt pavements, the temperatures at the surface–base interface and quarter-depth were found to be the most accurate representations of the effective pavement temperature for use in the proposed deflection correction methodology. Field validation demonstrated that the proposed methodology consistently outperformed the traditional AASHTO 1993 correction approach, offering a more accurate and practical solution for temperature correction in pavement structural evaluation.

17. Key Words	18. Distribution Statement
pavement evaluation, falling weight deflectometer, temperature correction, full-depth asphalt pavements, viscoelastic analysis, finite element modeling, machine learning; deflection basin	No restrictions. This document is available through the National Technical Information Service, Springfield, VA 22161.

19. Security Classif. (of this report)	20. Security Classif. (of this page)	21. No. of Pages	22. Price
Unclassified	Unclassified	49	

EXECUTIVE SUMMARY

Introduction

Pavement deflections measured with the falling weight deflectometer (FWD) are widely used to assess the structural condition of flexible pavements. However, these deflections are highly sensitive to pavement temperature during testing, especially in asphalt layers where stiffness can vary significantly with temperature. If temperature effects are not appropriately considered, interpretation of FWD data may result in inaccurate structural evaluations, potentially leading to improper design or maintenance decisions.

The Indiana Department of Transportation (INDOT) currently follows the temperature correction procedure recommended in the American Association of State Highway and Transportation Officials's (AASHTO) 1993 *AASHTO Guide for Design of Pavement Structures*, which applies a linear correction factor based on an effective asphalt temperature to normalize the central surface deflection (D0) to 20° C (68° F). However, this approach is limited in scope and accuracy, particularly under high temperature gradients or when interpreting deflections beyond the central sensor.

This study aimed to evaluate the adequacy of the AASHTO method for Indiana Department of Transportation (INDOT) pavements and to develop an improved temperature correction procedure that accounts for both surface and basin deflections. Field FWD testing was conducted across multiple pavement structures and environmental conditions, and the results were complemented with finite element (FE) simulations and a machine learning temperature prediction model to generate a robust correction framework.

Findings

- **Limitations of the AASHTO Method:** Field data confirmed that the AASHTO 1993 temperature correction tends to overcorrect deflections at high temperatures, especially for thick asphalt layers with steep thermal gradients. The method only adjusts D0 and ignores temperature effects on outer geophones, often resulting in unrealistic basin shapes and erroneous deflection basin parameters (DBPs).
- **Field and FE Analysis:** FWD testing on various pavement structures at different times of the day revealed clear relationships between pavement temperature and deflection changes. These relationships were further supported by FE models that simulated viscoelastic pavement behavior under controlled temperature inputs. The FE models helped fill gaps in field data, especially for temperature conditions not observed during testing.
- **Machine Learning-Based Temperature Prediction:** A machine learning model was developed to predict pavement temperatures at different depths based on readily available environmental inputs (average air temperature, pavement surface temperature, time of day, etc.). This tool allows accurate estimation of effective asphalt temperature without intrusive sensor installation, facilitating broader application of temperature correction procedures.
- **Development of Enhanced Correction Factors:** A comprehensive parametric study was conducted using calibrated FE models, accounting for variations in structural parameters. The resulting temperature correction factors were formulated using a unified, modified sigmoid function that integrates effective pavement temperature, asphalt layer thickness, and subgrade resilient modulus. Unlike traditional approaches, this novel method enables the correction of not only the central deflection, D0, but also outer deflections across the basin, thereby improving the accuracy of structural evaluations based on full deflection profiles.

Recommendations and Implementation

The results of this study indicate that temperature effects on FWD deflections should be addressed using a basin-wide correction approach rather than relying solely on the central-deflection adjustment in the AASHTO 1993 method. It is recommended that INDOT adopt the enhanced temperature correction procedure developed in this project, which adjusts both central and outer deflections based on effective pavement temperature, asphalt thickness, and subgrade stiffness. This approach provides a more reliable representation of the full deflection basin and improves the accuracy of subsequent structural evaluations.

For implementation, the new correction factors can be incorporated into INDOT's existing FWD analysis workflows with minimal modifications. Effective pavement temperature may be estimated using the machine-learning model developed in this study or from available surface and air temperature inputs. Incorporating these correction procedures into current post-processing tools will improve consistency and accuracy in structural evaluations, deflection basin parameters, and backcalculated layer moduli across project- and network-level analyses.

CONTENTS

LIST OF TABLES

LIST OF FIGURES

1. INTRODUCTION

1.1 Background

Pavement surface deflection, measured using the falling weight deflectometer (FWD), is a widely adopted nondestructive method for evaluating the structural condition of in-service flexible pavements. FWD data not only inform backcalculated moduli of pavement layers but also enable the computation of deflection basin parameters (DBPs), which are gaining traction as reliable indicators of pavement structural performance. For example, the study "Remaining Service Life Prediction of Indiana Pavements Using Mechanistic Methods" from Cho et al. (2025) confirmed the value of DBPs for characterizing the condition of Indiana Department of Transportation (INDOT)-maintained pavements and set the stage for their broader application in pavement management systems.

However, it is well established that asphalt pavement behavior is highly sensitive to temperature due to the viscoelastic nature of bituminous materials. As temperature increases, asphalt stiffness decreases, leading to larger measured deflections. Conversely, lower temperatures increase stiffness and reduce deflections. Because of this sensitivity, the raw FWD deflections recorded in the field must be normalized to a reference temperature—typically 20° C (68° F)—to enable consistent interpretation across geometric and environmental conditions.

INDOT currently employs the temperature correction method outlined in the American Association of State Highway and Transportation Officials's (AASHTO) 1993 *Guide for Design of Pavement Structures* (AASHTO, 1993). This approach uses an empirically derived correction factor based on an "effective" asphalt temperature to adjust the maximum central deflection (D0). However, several studies have demonstrated that this method often overcorrects deflections, especially at elevated surface temperatures (Kim et al., 1995). The primary limitations include using a single mean temperature, which does not adequately capture steep thermal gradients during heating or cooling cycles, and the narrow scope of the method, which corrects only D0 while neglecting other geophone offsets. This selective correction can result in physically unreasonable deflection basins, such as cases where D0 appears smaller than the deflection at 200 mm (8 in.) from the load center (D200), undermining the reliability of DBPs and subsequent structural assessments.

1.2 Research Need and Rationale

Temperature correction of FWD deflections is essential for accurate pavement evaluation, yet current methods fall short in accounting for the temperature-dependent response of asphalt layers. Although field FWD testing under varied temperature conditions provides some insights, it is limited by narrow thermal ranges and operational challenges.

To address these limitations, this study complements field testing with finite element (FE) modeling. Viscoelastic FE simulations enable exploration of pavement behavior across broader temperature scenarios and allow modeling of conditions difficult to replicate in the field. This integrated approach makes it possible to develop more robust correction models that account for temperature effects on multiple deflection points—not just D0—and under a broader range of environmental conditions. This enhanced correction procedure is expected to significantly improve the accuracy of backcalculated pavement moduli and the reliability of structural assessments conducted by INDOT.

1.3 Objectives

The primary objective of this study is to develop an improved temperature correction methodology for FWD deflections, aiming to minimize the influence of temperature variations on pavement structural evaluations. To achieve this objective, the following specific goals are established:

- Assess the applicability of AASHTO 1993 temperature correction factors to INDOT flexible pavements under current field conditions.
- Characterize the relationship between pavement temperature and FWD deflections, using both field-collected FWD data and results from FE simulations.
- Determine whether the identified relationships can be applied to adjust FWD deflections to a reference temperature, ensuring consistent results by minimizing temperature-related variability in field data.

1.4 Research Approach

To achieve the study's objectives, the research is structured into two main phases: (1) a field investigation and (2) numerical analysis using FE modeling. These phases are designed to assess the current temperature correction method's performance and develop an improved procedure tailored to Indiana's pavement conditions.

In a first phase, representative field sections were selected to reflect a broad range of flexible pavement structures commonly found across the INDOT network. FWD tests were conducted on each section under varying temperature conditions on the same day to minimize the influence of traffic loading and isolate the effect of temperature on measured deflections. Pavement cores were also extracted for laboratory characterization of material properties, which are essential inputs for the subsequent modeling phase. The collected FWD data was used to evaluate the AASHTO 1993 temperature correction procedure's performance and identify relationships between pavement temperature and deflection response for different structural configurations.

In a second phase, a viscoelastic FE model was developed for each pavement section using the material properties measured from field cores. The model was calibrated and validated against the field FWD data to ensure it reproduces pavement behavior accurately under measured temperature conditions. Once validated, the FE model was used to simulate pavement response over a wider range of asphalt thicknesses and temperature scenarios than those captured in the field. This parametric study allowed for the development of generalized deflection–temperature relationships applicable across various Indiana pavement types.

The outcomes of the field and modeling phases were integrated to formulate a new temperature correction methodology for FWD measurements. This updated approach aims to improve the accuracy of normalized deflections for all geophone positions—not just D0—and provide more reliable structural indicators for pavement evaluation.

2. LITERATURE REVIEW

2.1 Temperature Influence on Asphalt Pavement Deflections

A pavement's bearing capacity is defined as a structural state characteristic related to the capacity to support the expected traffic. Deflection is assumed to be one of the best indicators of structural capacity when evaluating bearing capacity. The FWD is one of the most widely used nondestructive testing (NDT) methods for evaluating it because it allows for applying different load levels with high accuracy and low dispersion in measured deflections (Kim & Park, 2002; B. Park, Cho, Rahbar-Rastegar, et al., 2023; Xiao et al., 2022). The FWD simulates moving wheel loads by applying impulse forces of 31, 40, and 49 kN (7,000, 9,000, and 11,000 lbf), with 40 kN (9,000 lbf) being the standard load used for analysis. It measures pavement surface deflections at nine locations using geophones arranged linearly from the center of the loading plate out to 1,500 mm (60 in.; Figure 2.1). Each deflection is labeled by its distance from the load center—for example, D600 corresponds to the deflection measured 600 mm (24 in.) away.

However, pavement deflection is affected by a variety of factors, such as loading factors (applicable load, circular load plate radius, and plate contact pressure), structural factors (number of layers, thickness, stiffness modulus, and Poisson's ratio), the temperature of the asphalt layers, gradients, discontinuities, and even variations in the general pavement structure (Strategic Highway Research Program [SHRP], 1993). Yet, among all influencing factors, temperature is widely recognized as the most critical and variable environmental factor affecting the mechanical behavior of asphalt layers and, consequently, the magnitude of measured deflections (Hu et al., 2022; Kim et al., 1995).

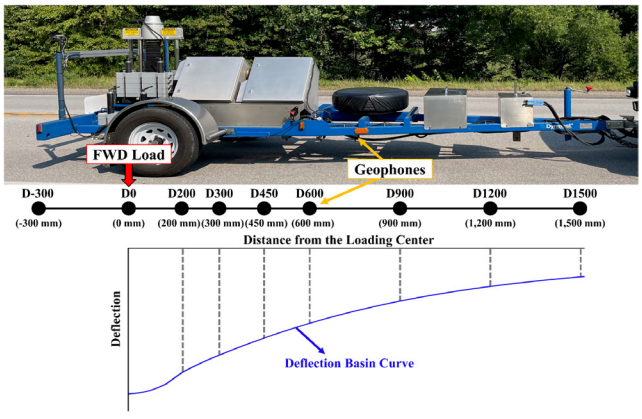

Figure 2.1 Schematic of FWD Geophones Locations and Deflection Basin Curve.

Asphalt is a viscoelastic material whose stiffness is highly temperature-dependent. At low temperatures, asphalt layers become very stiff (requiring greater force to deform), whereas at high temperatures the asphalt significantly softens and less force is needed to produce deformation (Lukanen et al., 2000). In short, a pavement's surface layer is much more rigid in cold conditions and more flexible in hot conditions, directly affecting how much a pavement deflects under load.

Temperature effects on pavement deflections are evident across both seasonal and daily timescales. Long-term studies show that FWD deflections are significantly higher in summer than winter, primarily due to reduced asphalt stiffness at elevated temperatures (Hu et al., 2022). In cold conditions—especially with frozen subgrades—pavement stiffness peaks and deflections are minimal, while in warmer months or during spring thaw, deflections increase due to both softened asphalt and moisture-weakened base layers (Pierce et al., 2017). These seasonal trends are mirrored on a daily scale: deflections measured in the early morning are typically lower and steadily rise as pavement temperatures increase throughout the day. Ramos García and Castro (2011) demonstrated this diurnal pattern by measuring FWD deflections from morning to afternoon, observing a consistent increase in deflection as surface temperatures climbed.

Pavement temperature is inherently nonuniform with depth, and this vertical gradient significantly affects asphalt stiffness and, consequently, FWD deflections. During typical diurnal cycles, the surface layer of asphalt heats and cools faster than the bottom, leading to positive or negative thermal gradients that create varying stiffness profiles throughout the layer (Kim et al., 1995; Zheng et al., 2019). Thicker pavements tend to exhibit more pronounced gradients due to their insulating effect (Han et al., 2024). As a result, a single uniform modulus cannot accurately represent the entire asphalt layer, especially under steep thermal gradients. FWD data confirm that temperature effects are most prominent near the load center, where deflection is governed by the asphalt response, while deflections at outer sensors—reflecting deeper layers—are largely insensitive to temperature (Straube & Jansen, 2009). These observations have led to the concept of an "effective influence radius," typically around 0.6 to 0.9 m (2 to 3 ft), within which temperature correction is necessary (Hu et al., 2022). To manage this complexity, engineers often use the mid-depth asphalt temperature as a representative value, supported by studies that show it correlates well with backcalculated moduli (Kim & Park, 2002; Noureldin et al., 2005). However, when thermal gradients are steep, even this simplification can introduce error, and advanced modeling approaches that incorporate actual temperature profiles yield more accurate deflection predictions.

Because asphalt stiffness varies significantly with temperature, interpreting FWD deflection data without considering pavement temperature can lead to erroneous conclusions about structural integrity. Elevated temperatures reduce asphalt stiffness and inflate deflections, which may be mistaken for pavement deterioration if uncorrected. To mitigate these effects, transportation agencies typically schedule FWD testing during moderate temperature conditions—commonly

between 18° C and 40° C (64° F and 104° F)—to minimize thermal variability. However, deflection measurements must be normalized to a standard reference temperature, usually 20° C or 25° C (68° F or 77° F), to ensure reliable and comparable evaluations. This correction process generally involves two steps: first, estimating the effective asphalt layer temperature using either embedded sensors or temperature prediction models (D.-Y. Park et al., 2001); and second, applying temperature correction factors to adjust the measured deflections accordingly (Pais et al., 2020).

In summary, accurate FWD analysis requires incorporating temperature effects, including daily and seasonal fluctuations, thermal gradients, and structural factors such as asphalt layer thickness (Inge & Kim, 1995). Proper correction practices ensure deflection data reflect actual structural conditions rather than transient thermal states, thereby improving the reliability of backcalculated moduli and comparative assessments across locations or periods.

2.2 Temperature Prediction Models

Temperature is widely recognized as the most influential environmental factor affecting pavement deflections, particularly in flexible pavements (Kim et al., 1995). Although direct temperature measurements using embedded sensors can provide accurate profiles, they are intrusive, costly, and impractical for widespread field applications. Therefore, prediction models that estimate asphalt layer temperature from accessible climatic data are preferred in practice. These models aim to capture the complex heat transfer process that governs pavement thermal behavior and can be broadly categorized into analytical, numerical, and empirical approaches (J. Chen et al., 2019; D.-Y. Park et al., 2001).

2.2.1 Analytical Models

Analytical models are based on the solution of the heat conduction partial differential equation under idealized boundary conditions. Early work by Barber (1957) applied sinusoidal functions to represent periodic surface temperature variation in semi-infinite masses. More recent methods, such as Green's functions (J. Chen et al., 2017), Laplace transforms (D. Wang, 2012), and finite integral transforms (Alawi & Helal, 2012), have allowed for multilayer pavement system analysis. However, these models require significant simplification of boundary conditions and are most accurate under controlled or theoretical conditions.

2.2.2 Numerical Models

Numerical models handle more realistic boundary conditions and complex geometries. Techniques such as the Finite Difference Method (FDM), Finite Element Method (FEM), and Finite Volume Method (FVM) are widely used. For example, Dempsey and Thompson (1970) implemented an FDM-based model to assess climate effects on pavements, which was later incorporated into the Enhanced Integrated Climatic Model (EICM) used in theMechanistic-empirical Pavement Design Guide (MEPDG) framework. FEM and FVM offer improved flexibility in simulating two-dimensional (2D) and three-dimensional (3D) heat flow but at the cost of higher computational resources (Alavi et al., 2014; J. Chen et al., 2016).

2.2.3 Empirical Models

Empirical models, in contrast, are based on statistical regression and are favored for their simplicity and ease of implementation (Gedafa et al., 2013; Inge & Kim, 1995; Ntramah et al., 2023). Traditional empirical models include the SHRP high-order polynomial model (Huber, 1994), the Texas and Idaho models (1-order and 7-term; Fernando et al., 2001; Kassem et al., 2020), and the widely used BELLS series (Lukanen et al., 2000), developed from more than 10,000 long-term pavement performance (LTPP) observations. These models use variables such as surface temperature, time of day, and recent air temperature history, but often tend to underestimate temperatures at high extremes and require local calibration to enhance accuracy (Ayasrah et al., 2023; J. Li et al., 2025; Y. Li et al., 2018). Furthermore, these models were generally developed using limited datasets or fixed-depth temperature measurements, reducing their general applicability.

Other efforts, such as the model proposed by Park et al. (2001), reduced the input requirements and addressed diurnal temperature effects but were less accurate for pavements with thicker asphalt layers. A more recent model introduced by Li et al. (2018) incorporated solar radiation as an input and improved predictions for full-depth asphalt pavements, but its practicality is limited due to the need for weather variables that are not always available.

Emerging studies have explored the use of machine learning (ML) techniques for predicting pavement temperature profiles. ML algorithms are capable of identifying complex, nonlinear relationships in large datasets and have been successfully applied in pavement engineering. For instance, models using artificial neural networks (ANN), random forests (RF), and other techniques have demonstrated strong predictive performance using LTPP and field-collected datasets (Abo-Hashema, 2013). Notably, Ghalandari et al. (2023) developed ML models trained on more than 370,000 temperature records using deep learning architectures such as autoencoders and long short-term memory (LSTM) networks. Although these models achieved high accuracy, they relied on extensive input variables—including solar radiation, humidity, and wind speed—which limits their practicality in many applications.

In summary, while empirical models remain the most practical for field use due to their simplicity, numerical and ML-based models offer greater accuracy and adaptability. The ideal choice depends on the availability of input data, computational resources, and required accuracy. Future research trends point toward hybrid models that combine physics-based principles with data-driven techniques for improved robustness and applicability across different pavement types and environmental conditions.

2.3 Temperature Correction Methods for FWD Deflections

Highway agencies typically adjust FWD deflections to a standard reference temperature (often 20° C or 68° F) so that pavement structural evaluations are comparable year-round (Kim et al., 1995; SHRP, 1993). For example, the AASHTO design guide specifies normalizing deflections to 20° C (68° F) because the asphalt layer's structural number is defined at that temperature. Temperature correction is especially critical for thick asphalt pavements, such as those used by INDOT, often higher than 200–300 mm (8–12 in.) of asphalt, because thicker asphalt layers exhibit a greater temperature dependency of deflections (Kim et al., 1995). This means that without correction, the structural capacity of a thick pavement could be severely under- or over-estimated in hot or cold conditions. This section summarizes the principal temperature correction methods, from empirical adjustments used in practice to mechanistic and advanced modeling approaches proposed in research.

2.3.1 Empirical Correction Methods

Empirical methods rely on observed correlations between pavement temperature and FWD deflections. Based on field data regressions, these methods produce formulae or factors to adjust measured deflections to a reference temperature. They are generally easy to apply and have been widely adopted by agencies for network- and project-level analysis. However, empirical methods may be limited in accuracy outside the range of data used to develop them. Key empirical approaches include the standard AASHTO procedure and improved formulas from later studies.

AASHTO's approach, first codified in the 1993 *Guide for Design of Pavement Structures*, is an empirical procedure using a linear correction factor based on an "effective" asphalt layer temperature. It includes two separate charts: one for pavements with a granular or asphalt-treated base (Figure 2.2a), and another for those with a cement- or pozzolanic-treated base (Figure 2.2b). Engineers can thus correct a field deflection at test temperature to the adjusted deflection at standard 20° C (68° F) by multiplying by the factor read from the curves (or equivalent equation), yielding the normalized deflection.

While the AASHTO 1993 method is straightforward and easy to apply, several limitations have been identified. First, the method applies correction exclusively to D0, even though deflections at other radial distances—such as D200, D300, or D450—are also influenced by temperature (Hugo et al., 2001; Kim & Park, 2002). This can lead to unrealistic deflection basins, where corrected D0 values fall below those of more distant sensors, resulting in misleading DBPs and inaccurate back-calculated layer moduli. Second, the method does not clearly specify which pavement temperature should be used as input. As a result, transportation agencies commonly use surface temperature for convenience, even though it may not accurately reflect the thermal condition of the asphalt layer, particularly when temperature gradients are present due to diurnal heating and cooling cycles. Furthermore, Kim et al. (1995) demonstrated that under such conditions, the AASHTO 1993 method tends to overcorrect FWD deflections, especially at elevated surface temperatures—for example, > 38° C (> 100° F)—due to its reliance on a single average temperature that does not capture vertical gradients. These issues are further exacerbated in thick pavements, which can exhibit strong through-depth temperature gradients that fall outside the original asphalt layer thickness range of the method—up to 300 mm (12 in.). As a result, the procedure often produces unconservative estimates of pavement strength, as confirmed by field validations from Kim et al. (1995), and has prompted the development of more robust and accurate empirical models.

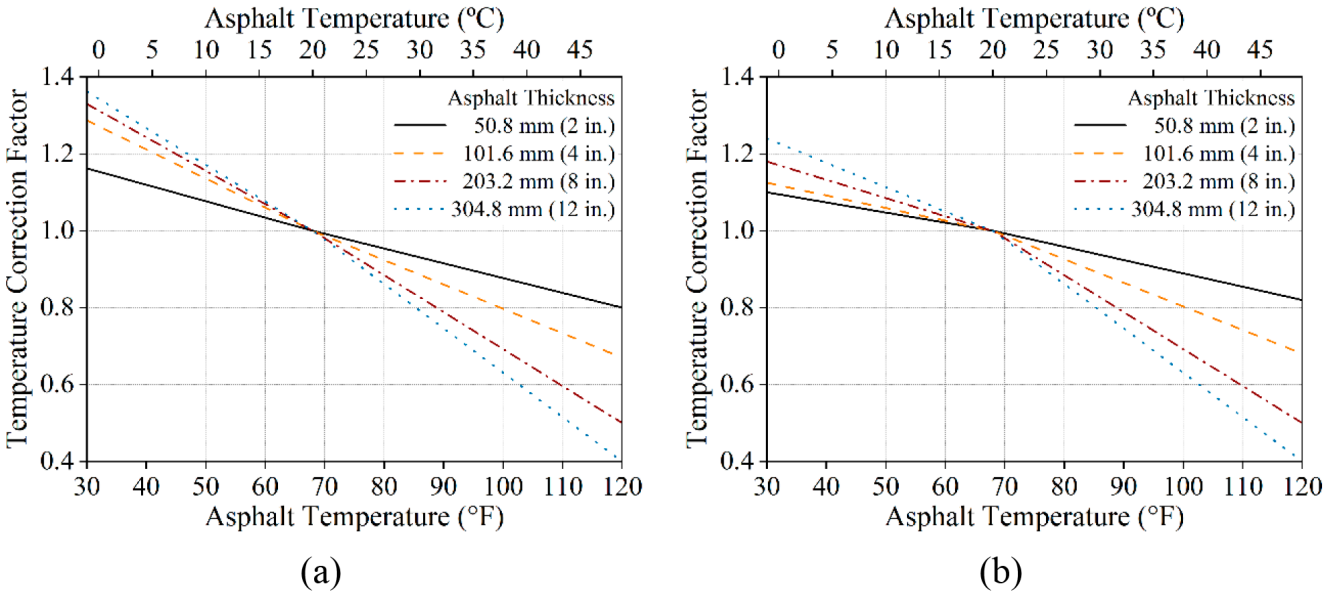

Figure 2.2 Temperature Correction Factors for D0 Deflections According to AASHTO 1993: (a) Granular and Asphalt-Treated Base, and (b) Cement- or Pozzolanic-Treated Base.

Later research developed improved empirical correction equations to address shortcomings of the original AASHTO method. It is worth mentioning the work of Kim et al. (1995) under the SHRP/LTPP program, which introduced a nonlinear temperature correction formula. Kim's method is based on the finding that the mid-depth asphalt temperature is the most effective single indicator of asphalt layer stiffness for deflection correction. The relationships between FWD deflection and mid-depth temperature were found to be nonlinear, and Kim et al. (1995) formulated an exponential correction model:

$$D_{68} = 10^{\alpha(68-T)} \cdot D_T \tag{2.1}$$

where D_T is the deflection measured at asphalt mid-depth temperature T (° F) and D_{68} is the deflection normalized to 20° C (68° F). The key parameter α is an empirically determined coefficient that depends on the asphalt layer thickness. For wheel path measurements, Kim et al. (1995) found $\alpha = 3.67 \cdot 10^{-4} \cdot t^{1.4635}$ (with t meaning the thickness of the asphalt layer in inches), while for lane-center measurements (between wheel paths), a similar α with a slightly different exponent is used. This thickness-dependent factor means the model predicts a larger temperature correction for thicker pavements, consistent with the reality that deflections on thick asphalt sections change more with temperature than on thin ones. In effect, the thicker the asphalt layer, the greater the correction factor α, reflecting higher temperature sensitivity.

This mid-depth exponential model offers significantly improved accuracy over AASHTO's linear method, particularly at higher temperatures. Using mid-layer temperature and a nonlinear form incorporating asphalt thickness reduces deflection correction errors and improves consistency across test locations. Widely adopted by highway agencies and the LTPP program, this method remains simple enough for routine use while offering better scalability for thick pavements. However, as an empirical model initially calibrated to North Carolina pavements, it may require local calibration to different climates or materials, and it does not account for moisture or other seasonal effects. Also, Kim's model is effective for adjusting D0 but insufficient for full-basin correction.

Several refined empirical and semiempirical models have expanded on early correction approaches. Lukanen et al. (2000) introduced the BELLS2 and BELLS3 models to estimate mid-depth asphalt temperatures from surface readings, enabling practical application of correction methods such as Kim's. More recently, Hu et al. (2022) proposed a method to correct the entire FWD deflection basin using a "deflection change rate" based on the deflection at 200 mm (8 in.) radial distance (D200), rather than correcting only D0. This approach yielded improved accuracy for semi-rigid pavements and reflects a broader trend toward multi-parameter regression models that better capture the complete deflection basin response under temperature changes.

2.3.2 Asphalt Modulus Adjustment Models

Various researchers and agencies have implemented modulus-based temperature correction procedures based on the above concept. The general strategy is: determine the in-situ asphalt layer modulus at test temperature from FWD data, adjust that modulus to a reference temperature using a mechanistic model, then use the adjusted modulus to predict the deflection (or directly adjust the deflection). This procedure can be done with closed-form solutions or numerical methods. For example, the Texas Department of Transportation's Modulus Temperature Correction Program (MTCP) uses this approach to predict seasonal changes in pavement strength (Fernando et al., 2001). It adjusts backcalculated asphalt moduli to the reference temperature, accounting for temperature and loading frequency. By inputting a reference temperature (20° C or 68° F), the software reduces or increases the asphalt modulus from its field value according to an asphalt stiffness model. The adjusted modulus can then be used in layered elastic equations to compute normalized deflections or directly in design checks.

Despite offering a more mechanistic foundation, modulus-based temperature correction methods present several limitations. These approaches require accurate input data, including precise pavement layer thicknesses, asphalt temperatures at the time of testing, and reliable backcalculated moduli—each of which can introduce uncertainty if poorly measured or estimated. Additionally, the method depends on an assumed asphalt modulus–temperature relationship, which may not represent local materials unless properly calibrated. Errors in the initial backcalculation process can also propagate through the correction, compromising the accuracy of the final normalized deflection. Due to their complexity and data requirements, such methods are often impractical for network-level applications and are better suited for detailed project-level evaluations. Furthermore, they focus solely on temperature effects, neglecting other environmental influences such as moisture variation or freeze–thaw cycles, which may also impact deflection behavior.

2.3.3 Mechanistic-Empirical (M-E) Advanced Models

Recent research has trended toward combining mechanistic understanding with statistical modeling to improve temperature corrections. These can be viewed as "advanced" models that incorporate multiple parameters (thickness, material properties, subgrade strength, etc.) in a regression or algorithmic model.

One example is the work by Pais et al. (2020), who developed a comprehensive model to adjust FWD deflections to a reference temperature by considering several pavement characteristics simultaneously. Their model considers the asphalt layer thickness, subgrade stiffness, the FWD load level, and even the spacing of the FWD sensors (which influences basin shape) as input variables, alongside the pavement temperature. The result is an equation that yields a temperature adjustment factor tailored to the specific pavement structure and condition. In effect, it is a multivariable regression built on a mechanistic foundation. Pais et al. (2020) validated this model on data from hot and temperate regions, showing it can improve accuracy over single-factor methods for various pavement types. A model such as this is well-suited for thick pavements, as it explicitly uses thickness and can be calibrated for the higher subgrade moduli

or different load responses under thick sections. The trade-off is complexity: an agency would need to measure or estimate multiple inputs (e.g., backcalculate subgrade modulus, etc.) and apply a complex formula.

Another advanced approach is to leverage the complete deflection basin data and machine learning or optimization techniques. The study by Hu et al. (2022) mentioned earlier falls in this category, using basin shape parameters (deflection ratios) to correct each sensor's deflection. Some researchers have also explored FE modeling combined with regression: for instance, running viscoelastic finite element simulations of FWD tests at various temperatures on a given pavement structure, then using the results to train a simplified predictive model for deflection correction. These approaches can capture nonlinear temperature effects more accurately, including how temperature gradients (surface vs. bottom of a thick asphalt layer) influence the deflection bowl.

Advanced temperature correction models offer high accuracy and adaptability by incorporating multiple inputs and structural differences, making them especially useful for thick asphalt pavements and varied climatic conditions. However, their complexity, data requirements, and limited adoption by agencies pose challenges. Most remain research-level proposals, and their use demands technical expertise and caution to avoid misapplication. Despite these drawbacks, they represent a promising direction for future FWD correction methods.

3. EVALUATION OF AASHTO 1993 TEMPERATURE CORRECTION FACTORS

3.1 Introduction

This chapter evaluates the performance of the AASHTO 1993 temperature correction method using both experimental and numerical FWD data. FWD tests were conducted on three pavement sections at two distinct temperatures on the same day to isolate the effect of temperature without introducing changes in pavement conditions. Material properties obtained from field cores were used to construct an FE model. The model was validated with field data and employed to perform a parametric study under varying subgrade conditions and temperature gradients.

3.2 Field FWD Deflection Data Collection

This study utilized two sources of FWD deflection data: (1) field measurements obtained from in-situ testing, and (2) simulated data generated through FE modeling. Field data were collected from three full-depth asphalt pavement sections in Indiana, each tested at two distinct temperature conditions on the same day to minimize structural changes. It should be noted that the surface temperature used for temperature correction was measured using the infrared sensor embedded in the FWD device (standard practice). Three test points were selected for each section, and deflections under a 40 kN (9,000 lbf) load level were recorded. The selected sections included a state route (SR 42), a U.S. highway (US 31), and an interstate highway (I-69). The corresponding asphalt thicknesses and testing temperatures are summarized in Table 3.1.

TABLE 3.1
Field Sections Description and FWD Testing Temperatures.

Section	Total Asphalt Thickness (mm)	Testing Location	Low Testing Temperature (° C)	High Testing Temperature (° C)
	362	A1	28.33	48.17
A (SR 42)	317	A2	26.89	47.83
	311	A3	26.89	52.39
	571	B1	25.56	56.06
B (US 31)	539	B2	25.17	56.50
	596	B3	25.33	56.11
	355	C1	12.89	16.50
C (I-69)	350	C2	12.78	16.06
	350	C3	12.83	15.67

3.3 Model-Based FWD Deflection Data

3.3.1 Pavement Structure

To supplement the field data and investigate temperature effects under controlled conditions, a FE model was developed using the software Abaqus. Section C (I-69) was selected for model development due to its recent construction, which ensured consistent pavement structure and the availability of high-quality cores for laboratory testing.

The pavement structure modeled consists of three asphalt layers—surface, intermediate, and base—placed over a thick subgrade layer. The layer thicknesses were determined from the field cores, and dynamic modulus tests were performed on specimens from each asphalt layer to measure their viscoelastic behavior. These properties were incorporated into the model through a Prony series formulation to represent time-dependent material response under loading. The subgrade was modeled as an elastic material, with three stiffness levels—elastic moduli of 35, 138, and 308 MPa (5, 20, and 45 ksi)—selected to evaluate the influence of subgrade support on deflection sensitivity to temperature. A subgrade thickness of 25,400 mm (83 ft) was used to minimize boundary effects (B. Park, Cho, Rahbar-Rastegar, et al., 2023). Table 3.2 presents details of pavement structures used for FE model development.

3.3.2 Model Description

Figure 3.2a shows the FE model developed from the structural information presented in Table 3.2. An axisymmetric model was adopted, which is commonly used in pavement analysis

TABLE 3.2
Description of the Pavement Structure (Section C) Used for FE Model Development.

Layer	Thickness (mm)	Modulus (MPa)	Poisson's Ratio
Asphalt surface	38.1	Dynamic modulus	0.35
Asphalt intermediate	63.5	Dynamic modulus	0.35
Asphalt base	254	Dynamic modulus	0.35
Subgrade	25,400	Elastic modulus: 308, 138, and 35	0.45

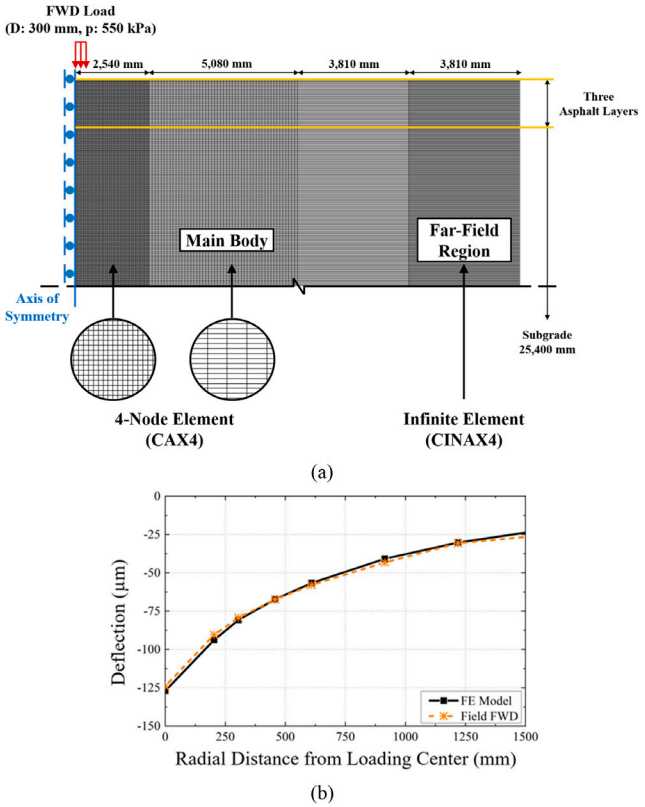

Figure 3.1 Details of the FE Model: (a) Designed FE Model, and (b) Validation of the FE Model.

to simulate circular FWD loading efficiently while maintaining accuracy (M. Li et al., 2017; B. Park et al., 2022; Yang et al., 2020). The model used four-node axisymmetric elements (CAX4) for the main body and infinite elements (CINAX4) at the outer boundaries. The mesh was refined in the loading and sensor zones to improve response accuracy. Boundary conditions included a fixed bottom and roller conditions along the axis of symmetry. A half-sine load with a 30 Hz frequency and a peak pressure of 550 kPa (80 psi) was applied over a circular plate with a 300 mm (12 in.) diameter, representing the FWD load. The model outputs were collected at the time of peak load, capturing the viscoelastic response of the asphalt layers under time-dependent loading conditions consistent with FWD field testing. The model was validated by comparing the computed deflection basin to the field measurements from Section C (I-69), showing a close match (Figure 3.2b).

3.3.3 Viscoelastic Material Properties

Once validated, the model was used for a parametric study using varying pavement temperature profiles and subgrade stiffness. Seven temperature gradient scenarios were simulated, including one with a uniform temperature of 20° C (68° F), used as a reference, and six additional cases based on the BELLS3 model (Figure 3.3). BELLS3, expressed in Equation (3.1), is an empirical model used to estimate pavement temperature at

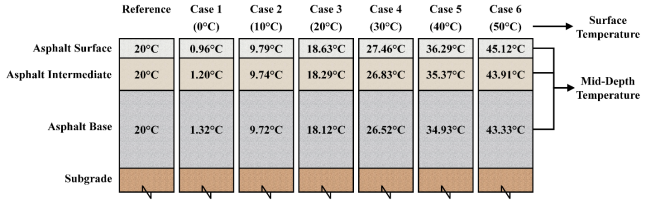

Figure 3.2 Temperature Gradient Scenarios.

different depths based on surface temperature, previous day's air temperature, testing time, and depth (Lukanen et al., 2000; D. Wang, 2013). It should be noted that these cases of temperature gradients were selected to cover the range of asphalt pavement temperatures used for AASHTO 1993 temperature correction factors (Figure 2.2).

$$\begin{aligned} T_d &= 0.95 + 0.892 \times IR \\ &\quad + \{\log d - 1.25\} \\ &\quad \times \begin{Bmatrix} -0.448 \times IR + 0.621 \times (1 - day) \\ +1.83 \times \sin(hr_{18} - 15.5) \end{Bmatrix} \\ &\quad + 0.042 \times IR \times \sin(hr_{18} - 13.5) \end{aligned} \tag{3.1}$$

where, T_d = pavement temperature at depth d (° C), IR = infrared surface temperature (° C), d = depth at which mat temperature is to be predicted (mm), *1-day* = average air temperature the day before testing, *sin* = sine function on an 18-hr clock system, with 2π radians equal to one 18-hr cycle, hr_{18} = time of day in a 24-hr clock system.

For each scenario, the calculated mid-depth temperature of each layer was then used to assign corresponding viscoelastic material properties. From each asphalt layer, two small cylindrical specimens were prepared for dynamic modulus testing following AASHTO TP 132-19 "Determining the Dynamic Modulus for Asphalt Mixtures Using Small Specimens in the Asphalt Mixture Performance Tester (AMPT)." These specimens, measuring 38 mm (1.5 in.) in diameter and 110 mm (4.3 in.) in height, were trimmed from cores using a diamond wet saw and oriented perpendicular to the pavement surface, as shown in Figure 3.3.

The dynamic modulus tests (Figure 3.4a) were conducted using an Asphalt Mixture Performance Tester (AMPT) at three temperatures—4, 20, and 40° C (40, 68, and 104° F). Each

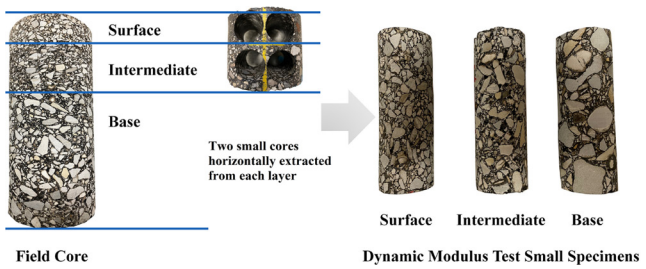

Figure 3.3 Small Specimens Preparation.

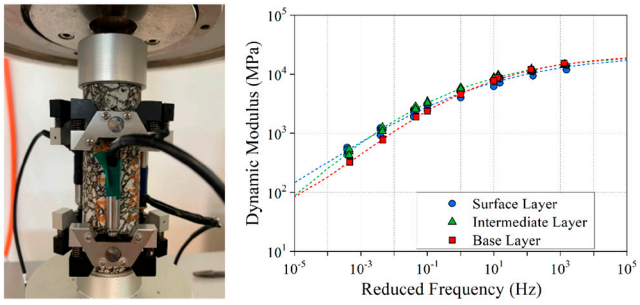

(a) (b)

Figure 3.4 (a) Dynamic Modulus Test Setup, and (b) Example of Dynamic Modulus Test Result for Section I-69.

specimen was subjected to cyclic axial loading at three frequencies (0.1, 1, and 10 Hz). Two replicate specimens per asphalt layer were tested under each condition. Load, time, temperature, actuator displacement, and deformation were recorded during testing. Deformations were monitored using three linear variable displacement transducers (LVDTs) positioned 120° apart around the specimen circumference to ensure accurate axial strain measurement.

The dynamic modulus data collected at various temperatures and loading frequencies were used to construct master curves by shifting the results to a reference temperature of 20° C (68° F). A sigmoidal function, Equation (3.2), was fitted to the data using nonlinear least squares optimization:

$$\log\left|E^*\right| = \log Min + \frac{\log Max - \log Min}{1 + e^{\beta+\gamma\log(\omega_r)}} \tag{3.2}$$

where *Min* and *Max* are the limiting minimum and maximum modulus values, with Max estimated using the Hirsch model and Min treated as a fitting parameter; β and γ are fitting coefficients, and ω_r is the reduced frequency (Hz).

Reduced frequency was calculated using the Arrhenius equation, obtaining a total of four fitting parameters during the optimization process:

$$\begin{aligned}\log(\omega_r) &= \log(\omega) + \log(a(T)) \\ &= \log(\omega) + \frac{\Delta E_a}{19.14714}\left(\frac{1}{T} - \frac{1}{T_r}\right)\end{aligned} \tag{3.3}$$

where ω is the loading frequency (Hz) at temperature T, $a(T)$ is the shift factor at temperature T, T_r is the reference temperature in Kelvin, and ΔE_a is the activation energy, treated as a fitting parameter. Master curves for each asphalt layer in section I-69 were developed and are shown in Figure 3.4b.

3.3.4 Prony Series Calculation

Asphalt mixtures exhibit viscoelastic behavior, meaning their response to loading is time- and temperature-dependent. To incorporate this behavior into the FE model, viscoelastic material properties were defined using a Prony series representation of the relaxation modulus, which describes how the material gradually relaxes under a constant strain.

To account for temperature effects, each asphalt layer was assigned a representative temperature (Figure 3.3). Dynamic modulus data obtained from lab testing at multiple temperatures and frequencies (Figure 3.4b) were shifted to each layer's mid-depth temperature using time-temperature superposition, enabling the calculation of a relaxation modulus *E(t)* for each layer. The relaxation modulus *E(t)* was defined by a generalized Maxwell model using a 10term Prony series:

$$E(t) = E_e\left(1 + \sum_{i=1}^{N} e_i e^{\frac{-t}{\tau_i}}\right) \tag{3.4}$$

where E_e is the long-term equilibrium modulus, namely the modulus as time t approaches infinity; e_i is the dimensionless relaxation modulus; τ_i is the relaxation time (with one-decade interval); N is the number of terms in the Prony series; and ν is the Poisson's ratio.

This form allows the viscoelastic behavior to be discretized into multiple relaxation mechanisms, each acting over a different time scale. The Prony series was fitted to dynamic modulus data by minimizing the least-squares error between the modeled and experimental storage and loss modulus curves. To use these properties in Abaqus, the relaxation modulus, *E(t)*, was converted into shear modulus, *G(t)*, and bulk modulus, *K(t)*:

$$G(t) = \frac{E(t)}{2(1+\nu)} \tag{3.5}$$

$$K(t) = \frac{E(t)}{3(1-2\nu)} \tag{3.6}$$

A constant Poisson's ratio $\nu = 0.35$ was assumed, which is a common simplification in viscoelastic analysis. These parameters enabled realistic time- and temperature-dependent behavior in the FE simulation.

When the time t approaches infinitesimal, the expression of the instantaneous modulus can be obtained as follows:

$$E_0 = E_e\left(1 + \sum_{i=1}^{N} e_i\right) \tag{3.7}$$

where E_0 is the instantaneous modulus, and e_i is the dimensionless relaxation modulus, both treated as fitting parameters. The number of terms N in the Prony series was selected as 10 in this study.

With the Fourier transforms, the relaxation modulus *E(t)* in the time domain can be converted to the complex modulus, $E^*(\omega_r)$, in the frequency domain as follows:

$$E^*(\omega_r) = E_0\left(1 - \sum_{i=1}^{N} \frac{e_i}{1 + i\omega_r\tau_i}\right) \tag{3.8}$$

where ω_r is the reduced frequency, dependent on temperature and loading frequency. The complex modulus was then

split into storage modulus, $E_s(\omega_r)$, and loss modulus, $E_l(\omega_r)$, representing the elastic and viscous components, respectively:

$$E_s(\omega_r) = E_0\left(1 - \sum_{i=1}^{N} \frac{e_i}{1+\omega_r^2\tau_i^2}\right) \tag{3.9}$$

$$E_l(\omega_r) = E_0 \sum_{i=1}^{N} \frac{e_i\omega_r\tau_i}{1+\omega_r^2\tau_i^2} \tag{3.10}$$

These frequency-domain moduli were used to validate the fit and ensure accuracy in reproducing each asphalt layer's measured dynamic modulus behavior.

This approach allowed temperature-dependent viscoelastic properties to be assigned layer by layer, using simplified but representative temperatures, which significantly reduced computational demands while still capturing the influence of realistic thermal gradients on FWD responses.

3.4 Effect of Temperature on Field FWD Deflections

Figure 3.5 presents the FWD test results for the three pavement sections introduced in Table 3.1. Square markers indicate measurements collected at lower temperatures, while circular markers represent those taken at higher temperatures. Solid lines correspond to uncorrected deflections, whereas dashed lines reflect D0 values corrected using the AASHTO 1993 method, which applies a correction based on asphalt surface temperature. This approach—relying on surface temperature measured

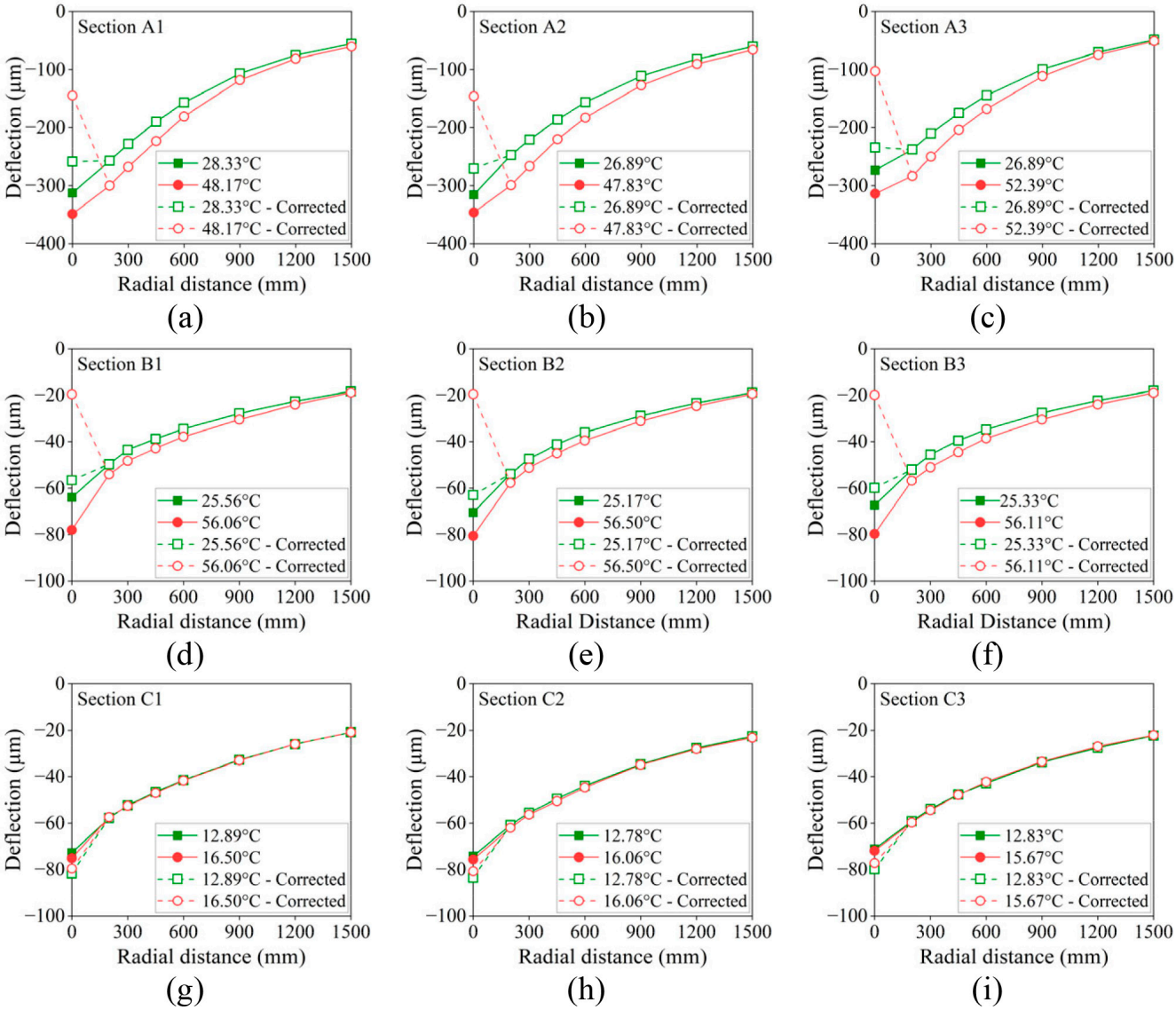

Figure 3.5 Effect of Temperature on the Field FWD Deflections of Testing Locations: (a) A1, (b) A2, (c) A3, (d) B1, (e) B2, (f) B3, (g) C1, (h) C2, and (i) C3.

by the infrared sensor on the FWD device—is commonly used by transportation agencies.

The data show that temperature influences not only the central deflection, D0, but also deflections at all sensor locations. This suggests that limiting temperature correction to D0, as done in the AASHTO 1993 method, does not fully account for the thermal effects on the entire deflection basin. Moreover, applying the correction to D0 did not yield consistent results across different temperatures. The corrected D0 values varied more than the uncorrected values in several cases. A general trend was observed in which corrected D0 values were lower at higher temperatures, which could lead to inaccurate evaluations of pavement structural conditions.

Comparing Sections A (Figure 3.5a to Figure 3.5c) and B (Figure 3.5d to Figure 3.5f), deflections in Section A were consistently higher, indicating a weaker structural response. Specifically, the differences in uncorrected D0 values between the two temperatures were 36.38, 30.72, and 40.32 μm (1.43, 1.21, and 1.59 mils) for points A1, A2, and A3, respectively, compared to 14.11, 10.14, and 12.46 μm (0.56, 0.40, and 0.49 mils) for B1, B2, and B3. Interestingly, while Section B had a higher average temperature difference between tests (30.87° C or 87.57° F) than Section A (22.09° C or 71.76° F), the deflection variation was more pronounced in Section A. This suggests that the absolute deflection level plays a key role in temperature sensitivity, which is likely influenced by pavement stiffness and the support conditions of underlying layers.

In the case of Section C (Figure 3.5g to Figure 3.5i), temperature had a smaller impact on the FWD results despite having deflection levels similar to Section B. This may be explained by the narrower temperature range in testing or the overall lower temperature levels. However, because field data under low temperature conditions were limited, additional analysis was carried out using numerical modeling to address this limitation.

3.5 Effect of Temperature on Model-Based FWD Deflections

Following the trends observed in the field data, which suggested that deflection magnitude could influence the temperature sensitivity, the FE simulations were designed to isolate this variable. To do so, three subgrade stiffness levels—35, 138, and 308 MPa (5, 20, and 45 ksi)—were evaluated, as shown in Table 3.2, while maintaining constant asphalt layer properties and thicknesses. This approach allowed for controlling overall deflection levels without altering the temperature-dependent behavior of the asphalt layers, which are primarily responsible for temperature sensitivity in FWD measurements.

Figure 3.6a, Figure 3.6c, and Figure 3.6e display model-based FWD deflection results for the three subgrade moduli under six pavement temperature gradient scenarios. Each graph also includes a reference case, where a uniform temperature of 20° C (68° F) was applied across all asphalt layers. Figure 3.6b, Figure 3.6d, and Figure 3.6f present the corresponding results after applying the AASHTO 1993 temperature correction method, using surface temperature for adjustment. The reference case was not corrected in these plots since it already reflects the standard condition. This analysis used absolute differences in deflection values to assess the impact of temperature, consistent with common engineering applications such as modulus backcalculation.

As expected, the deflection levels increased as subgrade stiffness decreased. More notably, the sensitivity of D0 to temperature also grew with higher deflection levels. For instance, the difference between D0 under 0° C and 50° C (32° F and 122° F) temperature gradients was 83.03 μm (3.27 mils) for the 308 MPa (45 ksi) subgrade model, but increased to 159.03 μm (6.26 mils) for the 35 MPa (5 ksi) case. Greater variations at sensors D1200 and D1500 were also observed in the low-stiffness subgrade model, indicating that deeper pavement responses are more affected under these conditions.

The corrected deflections in Figure 3.6b, Figure 3.6d, and Figure 3.6f reveal a reduction in the accuracy of the AASHTO 1993 method as deflection levels increase. In the stiffest subgrade model (308 MPa or 45 ksi), the spread between corrected D0 values remained relatively small (20.24 μm or 0.80 mils), while the model with the softest subgrade (35 MPa or 5ksi) showed a much larger discrepancy (141.56 μm or 5.57 mils).

These findings indicate that the AASHTO 1993 method may not sufficiently account for temperature effects, especially under high deflection level conditions. Since the method only adjusts D0 and ignores deflections at other sensor locations, it fails to capture the full influence of temperature on the deflection basin. The results further support the conclusion that both the magnitude of deflections (related to the pavement structure and condition) and the effective radial distance should be considered when developing more accurate temperature correction procedures.

3.6 Preliminary Investigation of the Effective Distance of Temperature Influence

The effective distance of temperature influence is defined as the radial distance from the load center within which pavement temperature significantly affects FWD deflections. This effect can be visually assessed in the model-based deflection results presented in Figure 3.6. As deflection levels increased (i.e., with lower subgrade stiffness), the temperature influence extended further from the loading point. For instance, in the case of the 308 MPa (45 ksi) subgrade (Figure 3.6a), deflection curves beyond the D900 sensor showed minimal variation with temperature, whereas in the 138 MPa (20 ksi) case (Figure 3.6c), temperature effects persisted up to D1200. For the lowest subgrade stiffness (35 MPa or 5 ksi, Figure 3.6e), even the farthest deflection measurement (D1500) displayed significant temperature sensitivity.

Figure 3.7 presents the absolute differences between the model-based deflections for each temperature gradient and the reference deflection values (obtained at 20° C or 68° F) for all sensor locations to quantify this trend. Figure 3.7a, Figure 3.7b, and Figure 3.7c correspond to the subgrade stiffness levels of 308 MPa (45 ksi), 138 MPa (20 ksi), and 35 MPa (5 ksi), respectively. Each line in Figure 3.7 represents a specific geophone, with the vertical axis showing the magnitude of temperature-induced deflection change relative to the reference condition.

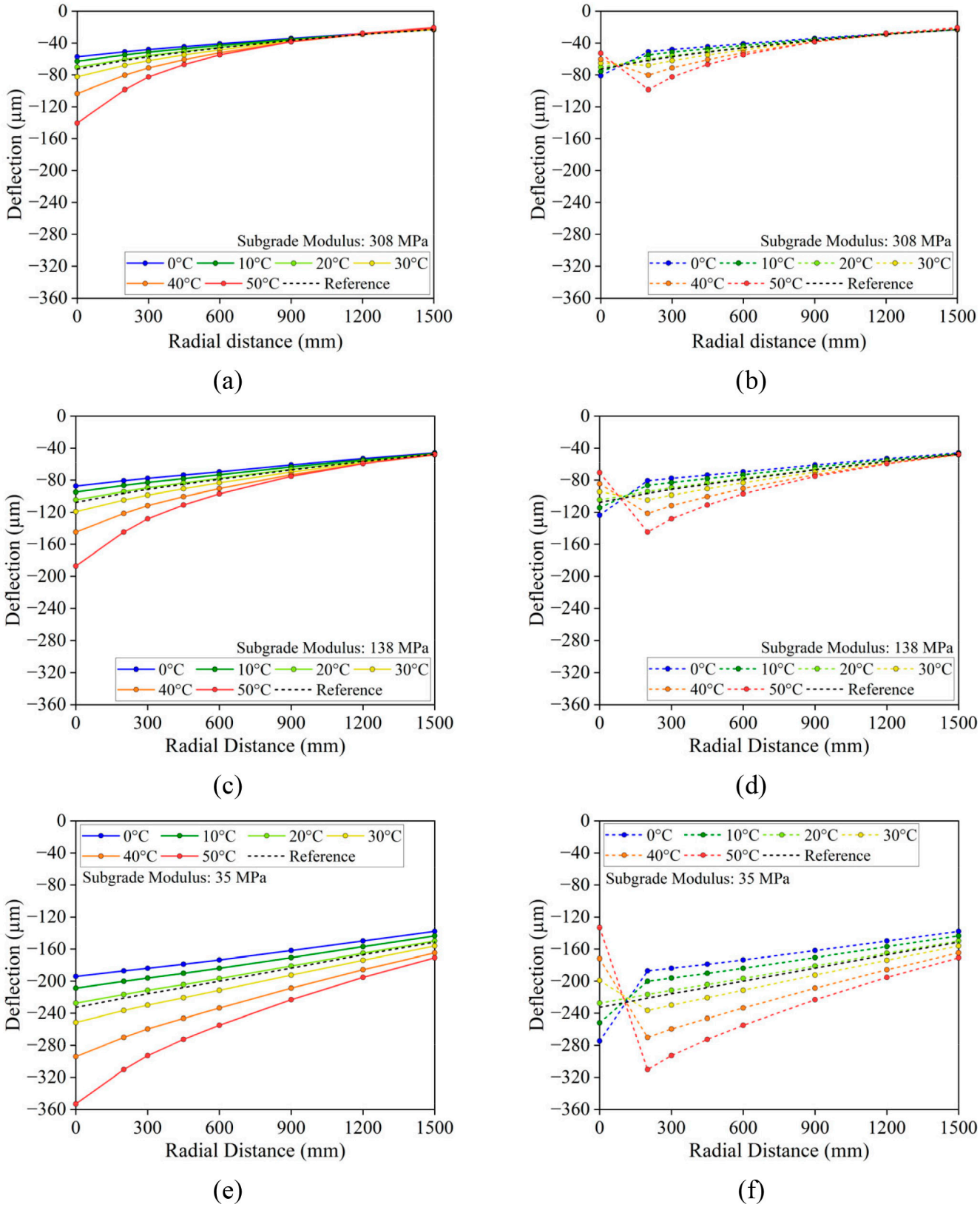

Figure 3.6 Comparison of Model-Based FWD Deflections at Three Levels of Subgrade Modulus Without Temperature Correction: (a) 308 MPa, (c) 138 MPa, and (e) 35 MPa, and After Temperature Correction Using the AASHTO 1993 Method: (b) 308 MPa, (d) 138 MPa, and (f) 35 MPa.

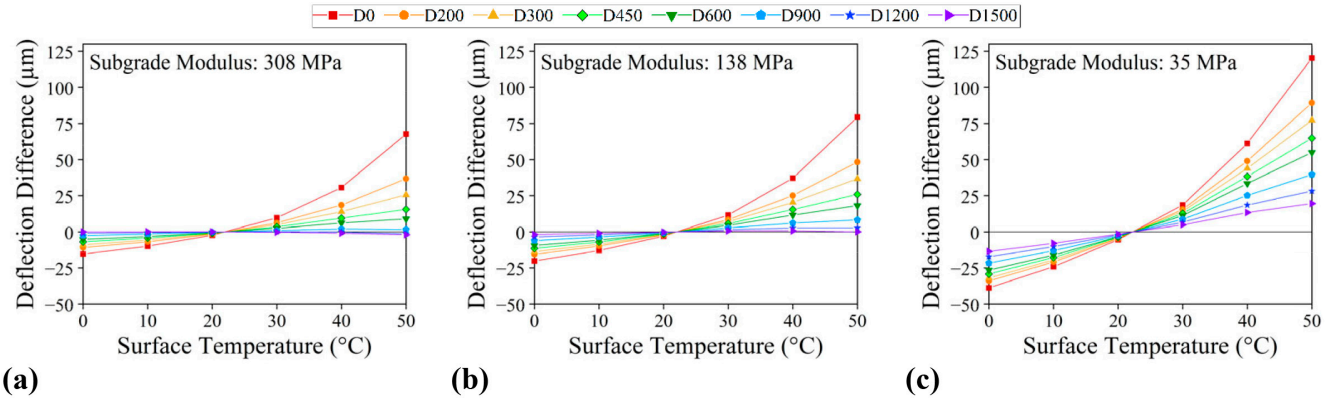

Figure 3.7 Differences Between Model-Based Deflection and Reference Deflection at Three Levels of Subgrade Modulus: (a) 308 MPa, (b) 138 MPa, and (c) 35 MPa.

As expected, the D0 sensor exhibited the greatest sensitivity to temperature. Moving radially outward, the deflection differences decreased, and the curves gradually flattened. The slope of each line reflects how sensitive the corresponding sensor is to temperature variations. In Figure 3.7a (308 MPa or 45 ksi), the D900 sensor curve becomes nearly horizontal, indicating that temperature influence beyond this point is negligible, thus establishing an effective distance of 900 mm (35 in.). In Figure 3.7b (138 MPa or 20 ksi), the effective distance extends to 1,200 mm (48 in.), as deflection differences remain appreciable up to that sensor. However, in Figure 3.7c (35 MPa or 5 ksi), none of the sensor curves reaches a horizontal profile, indicating that the temperature effect persists beyond 1,500 mm (60 in.).

These results clearly demonstrate that the effective distance of temperature influence increases with increased deflection level. Since higher deflections are associated with weaker pavement support or structural degradation, this finding suggests that both pavement condition and subgrade stiffness must be considered when defining temperature correction factors. Therefore, the assumption that temperature only affects the central deflection is insufficient, particularly for flexible or deteriorated pavement structures.

3.7 Summary

During this chapter, the influence of temperature variations on FWD deflections using both field measurements and model-based simulations was investigated. Field testing was conducted on three full-depth asphalt pavement sections, with deflections recorded at two distinct temperatures on the same day to isolate temperature effects. An FE model was developed using material properties obtained from field cores, allowing a parametric study with three subgrade stiffness levels and seven pavement temperature gradients. The AASHTO 1993 temperature correction method was also evaluated under these conditions. Key findings include:

- Both field and model-based deflections increased with rising temperatures, consistent with the thermal sensitivity of asphalt materials.
- In addition to temperature, the deflection level was found to significantly influence the magnitude of deflection variation. Pavements with higher deflection levels—due to thinner asphalt layers, lower bearing capacity, or deteriorated conditions—exhibited larger temperature-induced variations, even under moderate temperature differences.
- Deflection levels also impacted the effective distance of temperature influence, defined as the radial distance beyond which temperature no longer affects measured deflections. Higher deflection levels corresponded to longer effective distances.
- The AASHTO 1993 correction method, which corrects only D0 using surface temperature (standard practice), was shown to be inadequate in fully accounting for temperature effects. Other deflection sensors were also affected by temperature, and the accuracy of the correction method decreased with higher deflection levels.

These findings underscore the importance of considering deflection level and subgrade modulus, in addition to temperature, when correcting FWD data. Furthermore, relying solely on D0 corrections may lead to inaccurate interpretations of DBPs and overall pavement condition.

4. ESTABLISHMENT OF PAVEMENT TEMPERATURE GRADIENT PREDICTION MODEL WITH MACHINE LEARNING

4.1 Introduction

Accurate prediction of temperature gradients within asphalt pavements is essential for adjusting surface deflections and backcalculated layer moduli to reference conditions, given the temperature sensitivity of bituminous materials (Hermansson, 2002; Huang et al., 2024). Several models have been developed to estimate pavement temperatures and gradients, typically classified as analytical, numerical, or empirical (Adwan et al., 2021; Xu et al., 2017). While analytical and numerical models are grounded in heat conduction theory and can simulate multilayer systems, they often require complex input data, limiting their field applicability (J. Chen et al., 2019; D. Wang, 2013; Zheng et al., 2011).

Empirical models, including the widely used BELLS series (Lukanen et al., 2000), offer a more practical alternative by using surface and ambient temperature data. However, they tend to underestimate pavement temperatures under high-temperature conditions (> 40° C or 104° F) and often require local calibration to improve accuracy (Ayasrah et al., 2023; J. Li et al., 2025). More recent models have attempted to improve accuracy by incorporating additional climatic variables, such as solar radiation and wind speed (Y. Li et al., 2018), though these are not always available for routine pavement evaluations.

To overcome these limitations, recent research has explored ML techniques, which can capture complex, nonlinear temperature–depth relationships using large datasets. Algorithms such as ANNs, RF, and LSTM networks have shown promising results, particularly in thick asphalt and composite pavement systems (Ghalandari et al., 2023). However, most existing ML models rely on extensive weather data inputs, constraining their practical use.

This chapter investigates the development of simplified ML-based temperature gradient models tailored for two pavement types: full-depth asphalt and composite pavements. The goal is to achieve high predictive accuracy using only a limited, field-available set of input variables, enabling practical application in support of FWD deflection correction.

4.2 Data Collection

Temperature gradient data were collected from six pavement test sections in Indiana, including three full-depth asphalt pavements and three composite pavements (asphalt over rigid base). Each section was instrumented with temperature sensors embedded at various depths within the asphalt layers to capture vertical temperature distribution. The temperature sensors used were thermistors arranged in custom-designed bars, known as temperature trees (TT), as shown in Figure 4.1a.

Field measurements were conducted under various environmental conditions by performing FWD testing and simultaneous temperature readings during different seasons. In addition, hourly or bihourly temperature data were recorded during dedicated site visits to monitor thermal variation throughout the day. This approach enabled the capture of both seasonal and diurnal temperature effects across a range of pavement types. In total, 1,086 pavement temperature data points were collected across all sections.

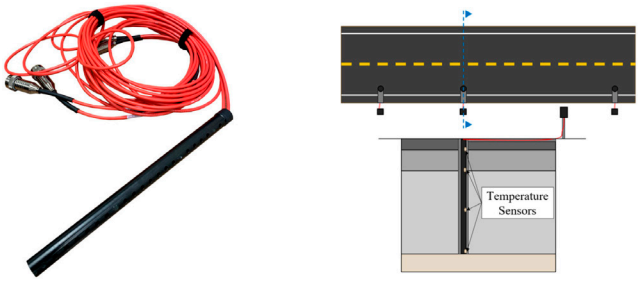

Figure 4.1 (a) Detail of a TT With 4 Temperature Sensors, and (b) Schematic Plan View and Cross-Section of the TT Setup in a Full-Depth Asphalt Pavement Section.

Sensor placement varied slightly depending on pavement type. For full-depth asphalt pavements, sensors were installed at the bottom of the surface and intermediate layers, with two to three additional sensors placed within the thicker asphalt base layer (Figure 4.1b). For composite pavements, four temperature sensors were embedded within the asphalt layer to monitor vertical gradients. Table 4.1 and Table 4.2 provide detailed sensor locations for each pavement type.

4.3 Empirical Models

To serve as baseline models for comparison with the machine learning (ML) approaches developed in this study, several established empirical models for pavement temperature prediction

TABLE 4.1
Temperature Sensor Placement in Three Full-Depth Asphalt Pavement Test Sections.

Test section	US 20	SR 42	US 31
Asphalt layer thickness (mm)	304.8	355.6	546.1
Number of sensor locations	3	3	3
Sensor depth (mm)	38.1, 101.6, 203.2, 292.1	38.1, 101.6, 228.6, 304.8	38.1, 101.6, 203.2, 419.1, 520.7
Sensor placement	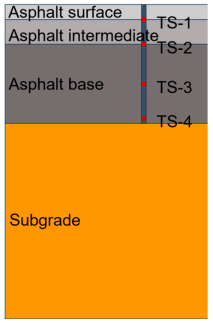	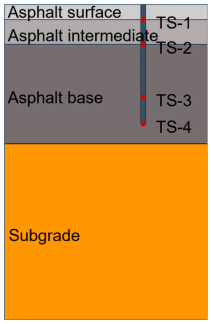	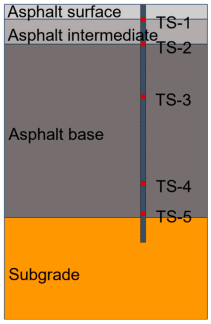

Note: TS represents Temperature Sensor

TABLE 4.2
Temperature Sensor Placement in Three Composite Pavement Test Sections.

Test section	SR 63	US 40	US 20
Asphalt layer thickness (mm)	139.7	241.3	292.1
Number of sensor locations	3	3	3
Sensor depth (mm)	25.4, 50.8, 88.9, 127	38.1, 101.6, 152.4, 203.2	38.1, 101.6, 177.8, 254

Sensor placement

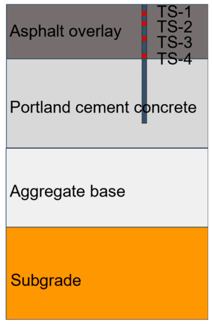

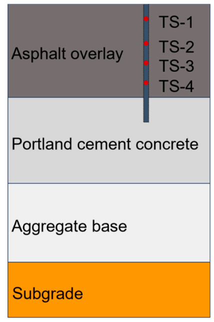

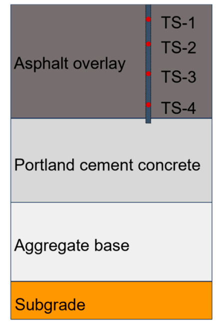

Note: TS represents Temperature Sensor

were selected. These include the BELLS3 model, the Texas model, the Idaho 7-term model, and Park's model.

4.3.1 BELLS3 Model

The BELLS3 model, commonly referred to here as the BELLS model, is one of the most widely used empirical models for predicting pavement temperature gradients. It incorporates the shade effect encountered during routine FWD testing and can be expressed mathematically as shown in Equation (3.1), defined in the previous chapter.

4.3.2 Texas Model

As an extension of the BELLS model, the Texas model (Fernando et al., 2001) incorporates regional calibration for Texas conditions, as shown in Equation (4.1), while maintaining the same input structure:

$$\begin{aligned}T_d &= 6.46 + 0.199\left(T_{surf}+2\right)^{1.5} \\ &+ \log(d)\Big[-0.083\left(T_{surf}+2\right)^{1.5} - 0.692\left(\sin\left(hr_{18}-15.5\right)\right)^2 \\ &+ 1.875\left(\sin\left(hr_{18}-13.5\right)\right)^2 + 0.059\left(T_{1-day}+6\right)^{1.5}\Big] \\ &- 6.784\left(\sin\left(hr_{18}-15.5\right)\right)^2\left(\sin\left(hr_{18}-13.5\right)\right)^2\end{aligned} \tag{4.1}$$

with all variables defined as in the BELLS model (see Section 3.3.3). Note that T_{surf} denotes the pavement surface temperature.

4.3.3 Idaho 7-Term Model

Developed as an alternative to the BELLS model using field data from Idaho, this model incorporates seven predictor terms and is expressed as shown in Equation (4.2):

$$\begin{aligned}T_d &= 6.46 + 0.199\left(T_{surf}+2\right)^{1.5} \\ &+ \log(d)\Big[-0.083\left(T_{surf}+2\right)^{1.5} - 0.692\left(\sin\left(hr_{18}-15.5\right)\right)^2 \\ &+ 1.875\left(\sin\left(hr_{18}-13.5\right)\right)^2 + 0.059\left(T_{1-day}+6\right)^{1.5}\Big] \\ &- 6.784\left(\sin\left(hr_{18}-15.5\right)\right)^2\left(\sin\left(hr_{18}-13.5\right)\right)^2\end{aligned} \tag{4.2}$$

This model is referred to simply as the Idaho model in the rest of the report.

4.3.4 Park's Model

Proposed by Park et al. (2001), this model was developed using data from six field sites in Michigan. It is notable for requiring fewer inputs and is expressed as shown in Equation (4.3). The only inputs are surface temperature, depth, and testing time:

$$\begin{aligned}T_d &= T_{surf} + \left(-0.3451d - 0.0432d^2 + 0.00196d^3\right) \\ &\sin\left(-6.3252t + 5.0967\right)\end{aligned} \tag{4.3}$$

where t is the time of testing in the range of 0 and 1 (days).

The above models were calibrated using the local Indiana dataset collected in this study to improve prediction accuracy under regional climatic conditions. A genetic algorithm was applied to optimize model coefficients using 80% of the dataset for training and 20% for validation.

4.4 Machine Learning Models

ML has become an increasingly valuable tool in civil engineering applications, particularly for modeling complex, nonlinear relationships that are difficult to capture with traditional

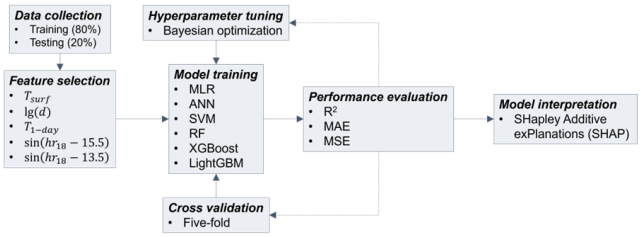

Figure 4.2 Workflow of ML Predictive Modeling.

statistical methods. In this study, six ML models were implemented to predict pavement temperature gradients, and their overall workflow is summarized in Figure 4.2.

4.4.1 Multivariate Linear Regression

Multivariate linear regression (MLR) is a basic yet interpretable approach that uses a linear function to model the relationship between a dependent variable and multiple independent variables. Although MLR is widely used for predictive tasks, its main limitation lies in its assumption of linearity, which may not hold in real-world pavement temperature scenarios with more complex input interactions.

4.4.2 Artificial Neural Network

An ANN, specifically a back-propagation neural network (BP-ANN), was employed to capture nonlinearities in the data. ANNs consist of interconnected layers of neurons—input, hidden, and output layers—that learn patterns by adjusting connection weights during training. This is accomplished via back-propagation, which minimizes prediction error through iterative updates. Although ANNs effectively handle nonlinear and multidimensional datasets, they require significant computational resources and training data.

4.4.3 Support Vector Machine

Support vector machine (SVM) is a supervised learning algorithm suitable for both regression and classification tasks (Hearst et al., 1998). In regression mode, it seeks to fit a function within a specified margin of tolerance while maximizing generalization. SVM can capture nonlinear relationships using kernel functions, which map inputs into higher-dimensional spaces. Although robust and resistant to overfitting, SVM can be computationally intensive for large datasets.

4.4.4 Random Forest

RF is an ensemble method that combines predictions from multiple decision trees to enhance robustness and accuracy (Breiman, 2001). Each tree is built on a bootstrapped sample of the data and uses a random subset of features. RF is known for its ability to reduce overfitting, handle noisy datasets, and quantify variable importance. It is effective for both small- and large-scale regression problems.

4.4.5 Extreme Gradient Boosting

Extreme gradient boosting (XGBoost) is a high-performance gradient boosting framework that constructs trees sequentially, with each new tree aiming to correct the errors of previous ones (T. Chen & Guestrin, 2016). It integrates regularization, missing data handling, and efficient parallelization to improve speed and accuracy. XGBoost is widely used in competitive data science because it balances performance and efficiency.

4.4.6 Light Gradient Boosting Machine

Light gradient boosting machine (LightGBM) is a gradient boosting algorithm designed for high efficiency and scalability (Ke et al., 2017). It employs a leaf-wise tree growth strategy, focusing on growing branches that significantly reduce loss. LightGBM supports large datasets with many features and is known for its fast training speed and low memory usage. It also includes advanced regularization mechanisms to minimize overfitting.

For all ML models, Bayesian optimization was used to tune hyperparameters efficiently. This method uses probabilistic models to explore the hyperparameter space more effectively than random or grid search methods. Additionally, five-fold cross-validation was employed to evaluate model generalizability and reduce bias in performance assessment. The dataset was split into 80% for training and 20% for testing, allowing a fair evaluation of model performance on unseen data.

4.5 Descriptive and Statistical Analysis

Temperature gradient data were collected from both full-depth asphalt and composite pavement sections over multiple seasons, using routine FWD testing as well as dedicated site visits. Simultaneously, associated weather information, such as the air temperature at the time of testing and the average air temperature from the previous day, was retrieved from publicly available meteorological sources.

Environmental conditions, especially solar radiation and wind velocity, are expected to influence surface pavement temperatures immediately. In contrast, deeper pavement layers respond more slowly to atmospheric temperature changes. This behavior was confirmed by the measured temperature gradients, as shown in Figure 4.3 and Figure 4.4 for both pavement types. As expected, surface temperatures displayed the most significant variability and reacted quickly to fluctuations in ambient air temperature. The surface temperature began to decline after reaching the daily maximum air temperature. In deeper layers, the magnitude of temperature fluctuation diminished, with lower layers typically recording higher temperatures than the surface during the early morning and evening, but lower temperatures during midday.

For full-depth asphalt pavements (Figure 4.4a), temperature variation with time becomes minimal at depths greater than approximately 420 mm (16.5 in.). In contrast, composite pavements with thinner asphalt layers exhibit temperature variation across the entire asphalt layer depth (Figure 4.4b).

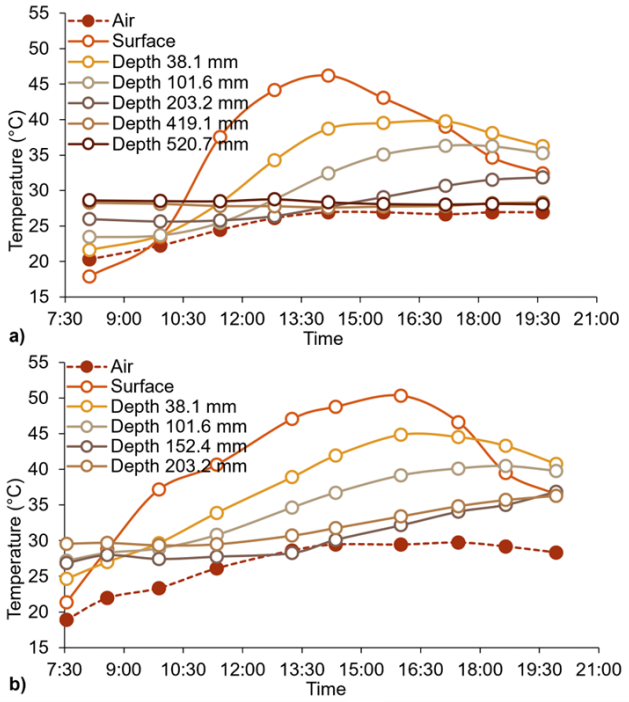

Figure 4.3 Variation of Pavement Temperature With Time at Different Layer Depths: (a) Full-Depth Asphalt Pavement, (b) Composite Pavement.

A total of 1,086 temperature data points were collected, encompassing a broad range of seasonal and diurnal conditions. These data were used for training and evaluating the predictive models. The key statistical properties of both input and output variables are presented in Table 4.3. The average air temperature on the day prior to testing ranged from approximately 0° C to 30° C (32° F to 86° F), aligning with the historical daily average air temperatures recorded in Indiana. Pavement temperatures at different depths varied between roughly 5° C and 50° C (41° F and 122° F), representing a total range of 45° C (113° F). This wide range of environmental and pavement temperature conditions enhances the generalizability of the predictive models developed in this study.

A correlation matrix of the input variables is presented in Figure 4.5 to explore potential dependencies between variables. The matrix includes scatter plots for each pair of variables and histograms showing their individual distributions. No strong correlations were observed among the input variables, indicating that they are statistically independent and appropriate for use in machine learning modeling. The data from full-depth asphalt and composite pavements were well balanced in terms of quantity and distribution.

4.6 Comparison Between Empirical and Machine Learning Models

The prediction performance of the empirical models (used as baselines) and the ML models was evaluated using the collected pavement temperature dataset. Initially, the BELLS3, Texas, Idaho 7-term, and Park's models were applied in their original forms to assess their predictive accuracy on the study data. To account for local climatic variations, all baseline models were subsequently recalibrated using 80% of the data for model fitting and 20% for validation. The same training and testing subsets were used for the ML models to ensure a fair comparison. Results are summarized in Figure 4.6 and Figure 4.7, and quantitative performance metrics are provided in Table 4.4, including the coefficient of determination (R^2), mean squared error (MSE), and mean absolute error (MAE).

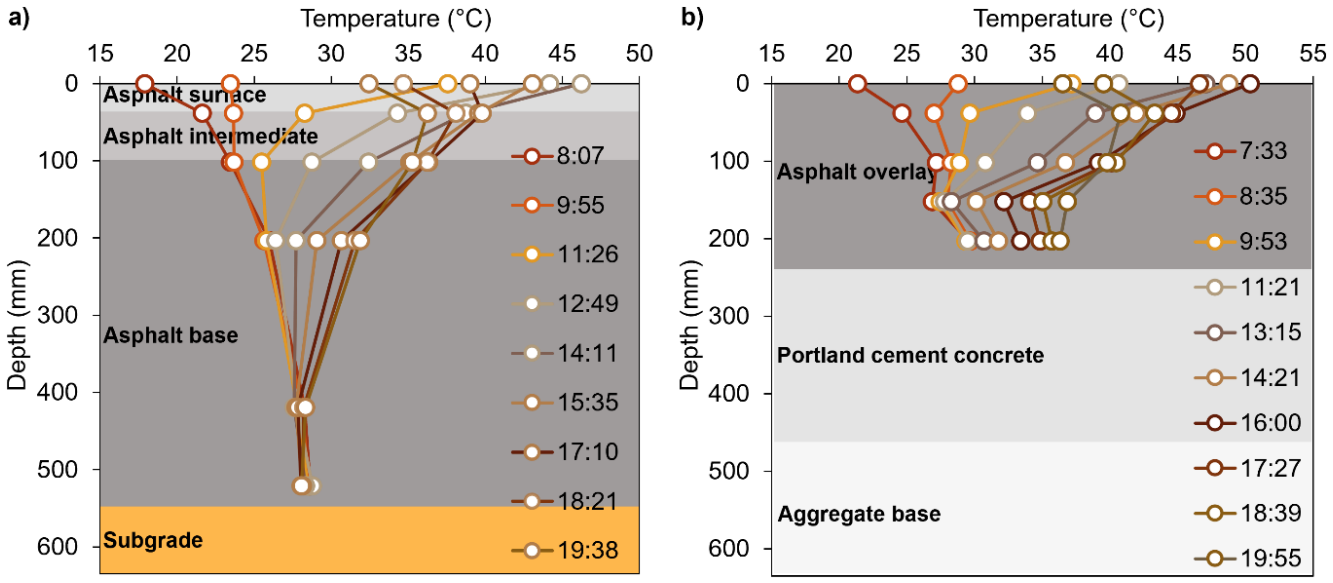

Figure 4.4 Variation of Pavement Layer Temperature at Different Times: (a) Full-Depth Asphalt Pavement, (b) Composite Pavement.

TABLE 4.3
Statistical Characteristics of Input and Output Variables.

Variables			Min.	Max.	Avg.	SD.
Input	Pavement surface temperature	T_{surf} (° C)	-0.389	60.056	34.121	13.199
	Asphalt layer depth (Log scale)	$\lg(d)$(mm)	1.405	2.717	2.056	0.365
	Average air temperature of the day before the testing day	T_{1-day}(° C)	1.4	28.889	21.498	6.228
	Time of the day during testing	$\sin(hr_{18}-15.5)$	-1	0.999	-0.470	0.660
	Time of the day during testing	$\sin(hr_{18}-13.5)$	-1	0.998	-0.135	0.716
Output	Pavement temperature at different depths	T_d (° C)	4.462	49.867	29.565	9.753

Notes: Min: Minimum; Max: Maximum; Avg: Average; SD: Standard Deviation

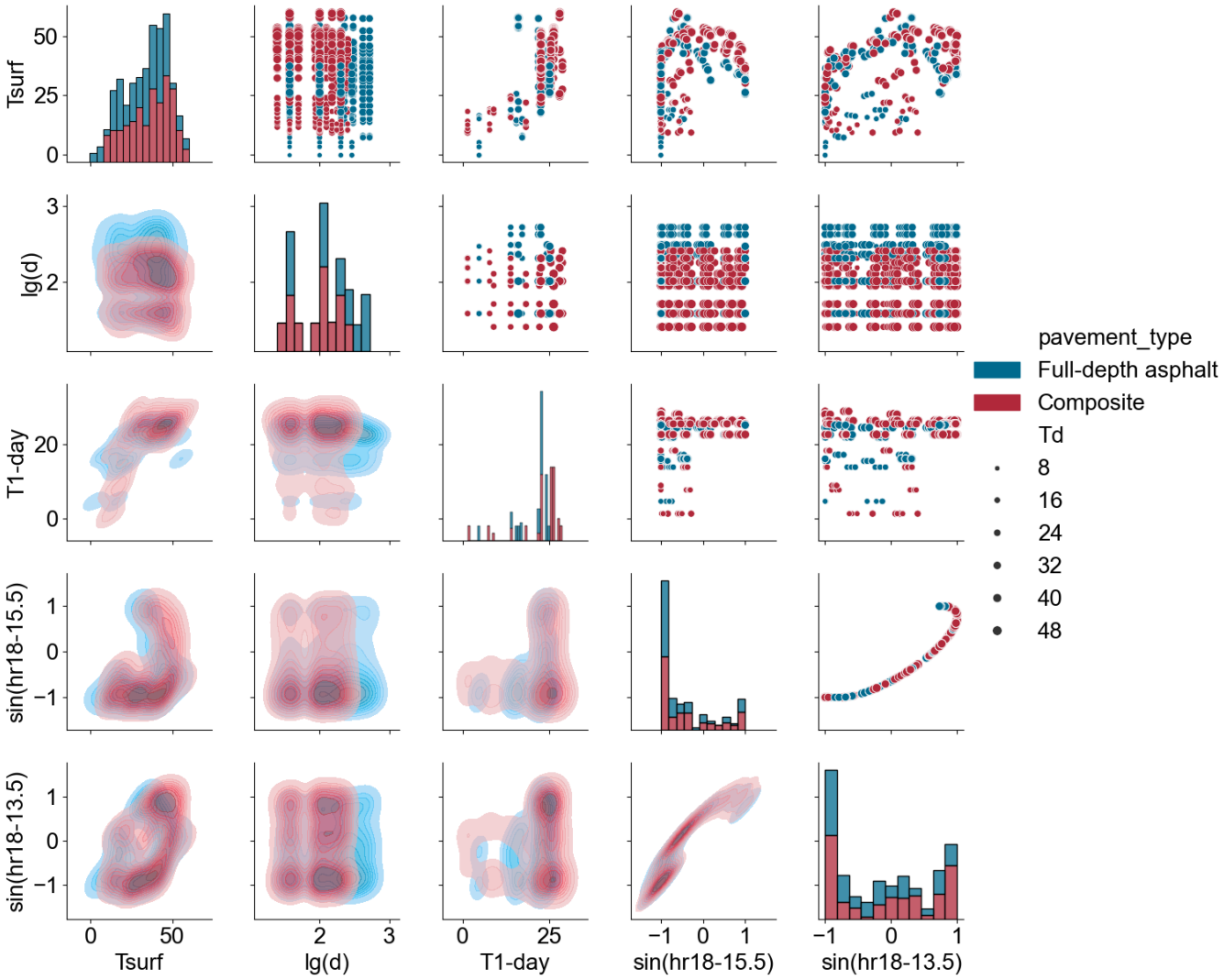

Figure 4.5 Correlation Matrix Plot of Input Variables.

The original BELLS3 model exhibited the highest predictive accuracy among the uncalibrated empirical models. Following local calibration, the Idaho 7-term model produced the best results, achieving an R^2 of 0.82 and an MAE of 2.85° C (5.13° F). In general, the performance of the baseline models improved after calibration, except for Park's model, which continued to show poor accuracy, likely due to its reduced number of input variables and simplified functional form.

In contrast, all ML models outperformed both the original and calibrated empirical models. Even the simplest ML

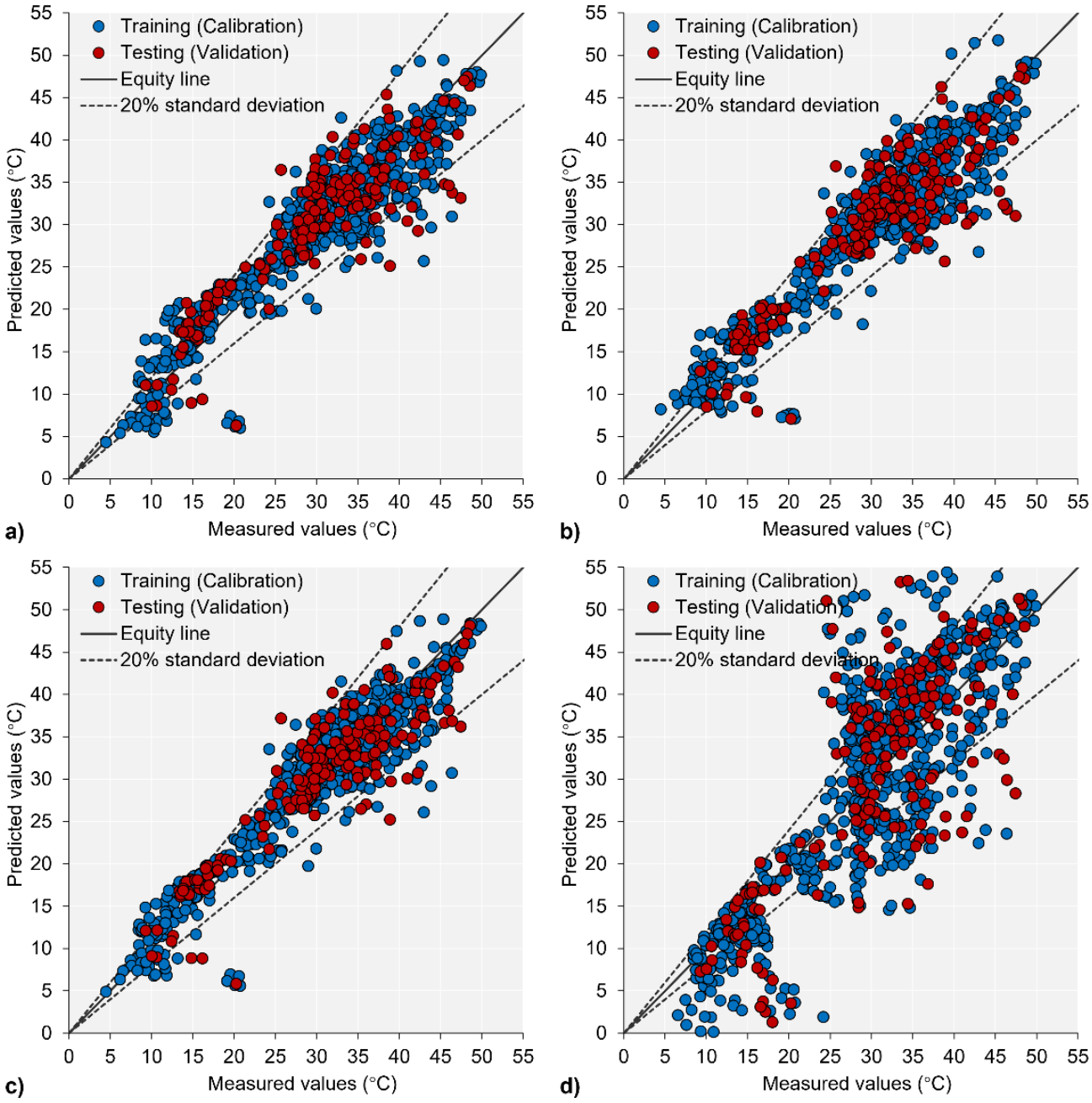

Figure 4.6 Calibration and Validation Results of Baseline Empirical Models, (a) BELLS3 Model, (b) Texas Model, (c) Idaho 7-Term Model, and (d) Park's Model.

approach, the MLR, provided better accuracy than most baseline models. This improved performance highlights the ML models' ability to capture complex, nonlinear relationships in the data that traditional models may not address. The ML algorithms benefited from hyperparameter tuning via Bayesian optimization, further enhancing their performance. Among the models, XGBoost achieved the highest accuracy, with an R^2 of 0.97, an MSE of 2.97, and an MAE of 1.18° C (2.21° F).

Figure 4.8 and Figure 4.9 illustrate representative examples comparing measured and predicted pavement temperatures across different depths and times of day. ML models, especially XGBoost, consistently outperformed the empirical models. While calibrated empirical models provided reasonable predictions, they generally showed reduced accuracy in composite pavements during early morning hours, as shown in Figure 4.9d. In contrast, the ML models maintained stable and accurate predictions regardless of pavement type or asphalt layer thickness.

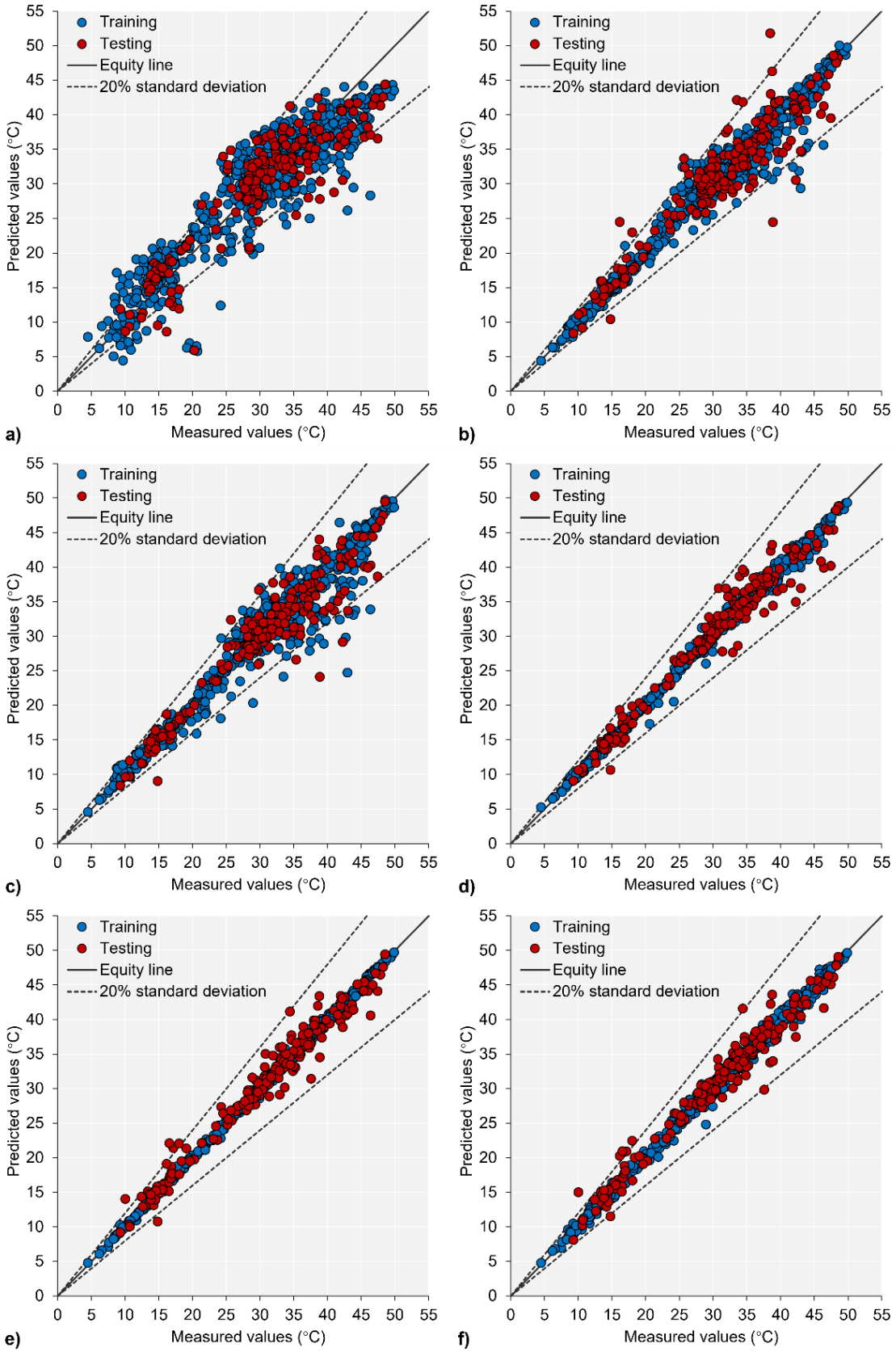

Figure 4.7 Training and Testing Results of ML Models: (a) MLR, (b) ANN, (c) SVM, (d) RF, (e) XGBoost, (f) LightGBM.

TABLE 4.4
Performance Metrics of Different Baseline Empirical Models and ML Models.

Model	Training/Calibration			Testing/Validation		
	R^2	MSE	MAE (° C)	R^2	MSE	MAE (° C)
Baseline models						
BELLS3 (Original)	**N/A**	**N/A**	**N/A**	**0.72**	**24.07**	**3.48**
BELLS3 (Calibrated)	0.86	13.60	2.80	0.79	18.22	3.14
Texas (Original)	N/A	N/A	N/A	0.65	29.62	4.16
Texas (Calibrated)	0.86	13.63	2.77	0.78	18.48	3.03
Idaho (Original)	N/A	N/A	N/A	0.44	48.33	5.28
Idaho (Calibrated)	**0.88**	**11.42**	**2.50**	**0.82**	**15.43**	**2.85**
Park's (Original)	N/A	N/A	N/A	-96.23	723.03	361.45
Park's (Calibrated)	N/A	N/A	N/A	0.72	24.07	3.48
ML models						
MLR	0.839	15.60	3.10	0.80	17.35	3.18
ANN	0.964	3.46	1.17	0.88	9.93	2.08
SVM	0.945	5.31	1.26	0.89	9.04	1.95
RF	0.995	0.47	0.44	0.95	3.95	1.32
XGBoost	**0.999**	**0.11**	**0.23**	**0.97**	**2.97**	**1.18**
LightGBM	0.995	0.44	0.49	0.96	3.19	1.26

Notes: N/A: Not Applicable

4.7 Feature Importance Analysis

To improve the interpretability of the ML models, SHapley Additive exPlanations (SHAP), an explainable ML method based on cooperative game theory, was employed. SHAP provides a consistent framework to evaluate the relative contribution of each input variable to the model's predictions by assigning Shapley values. These values quantify the marginal contribution of a feature across all possible combinations of inputs, offering a robust measure of feature importance.

SHAP analysis was applied to the XGBoost model, which showed the highest predictive performance among the tested ML models. Figure 4.10 presents the SHAP values for each input variable. Positive SHAP values indicate a positive contribution to the predicted pavement temperature, while negative values represent a negative influence. The magnitude reflects the strength of the effect.

Figure 4.10a shows that the "average air temperature of the previous day" ($T_{1\text{-}day}$) and the "pavement surface temperature" (T_{surf}) consistently had high positive SHAP values, highlighting their strong influence on model outputs. Figure 4.10b confirms that these two variables had the highest mean absolute SHAP values, making them the most significant predictors in the model.

In contrast, the variables representing the "time of day during testing" ($sin(hr_{18}$ *-15.5)* and $sin(hr_{18}$ *13.5)*) had relatively low SHAP values, indicating a limited direct impact. This is likely due to their indirect influence being captured by the

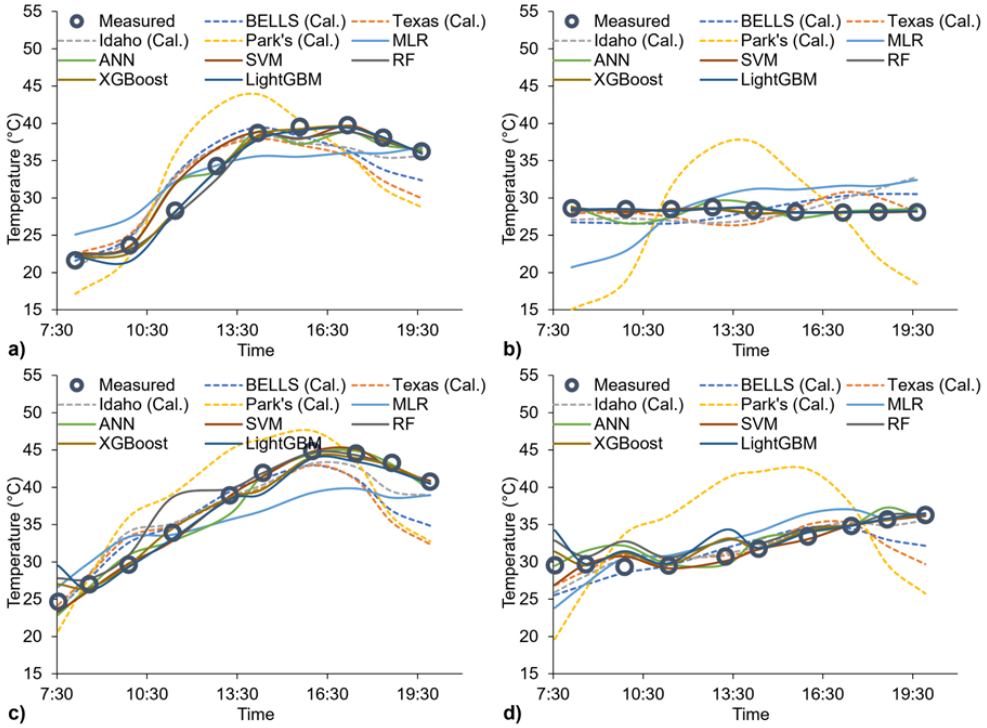

Figure 4.8 Measured Values Versus Predicted Values of Different Models in Terms of Time, Full-Depth Asphalt Pavement at the Depth of: (a) 38.1 mm and (b) 520.7 mm; and Composite Pavement at the Depth of (c) 38.1 mm and (d) 203.2 mm.

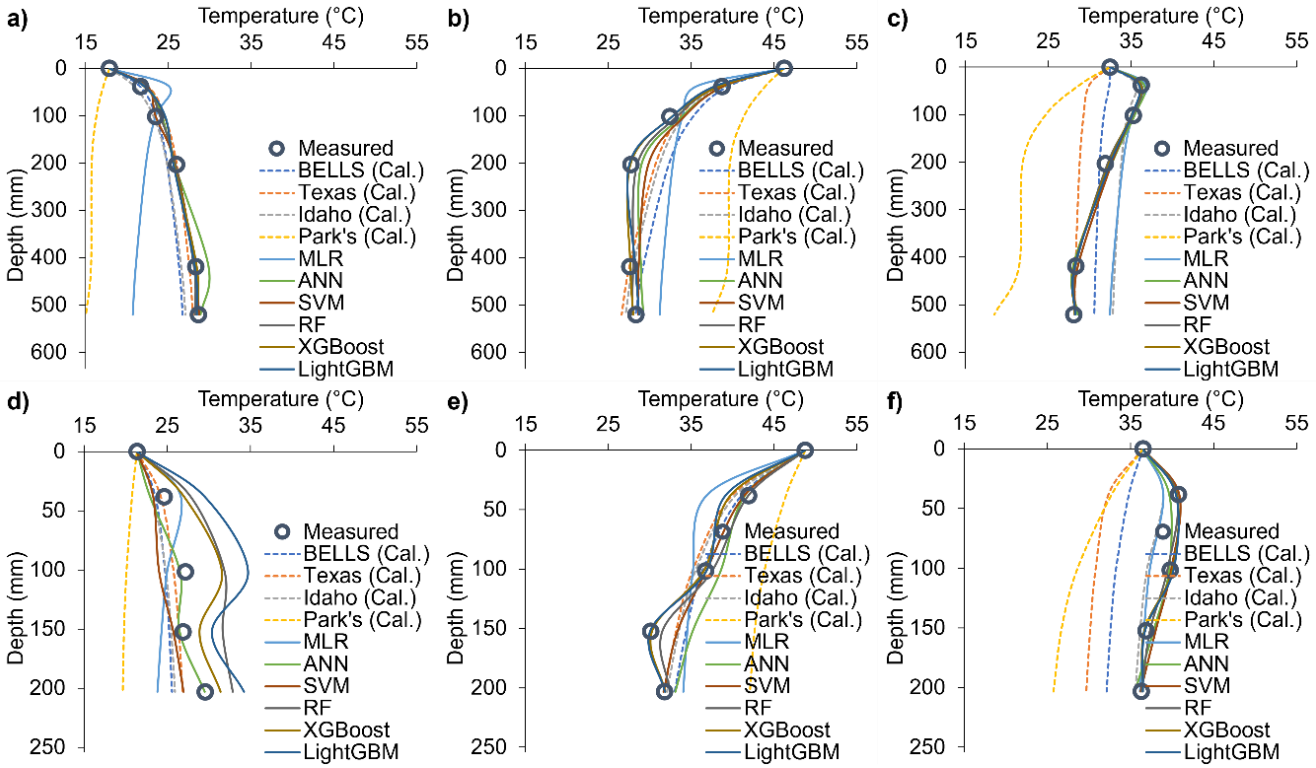

Figure 4.9 Measured Values Versus Predicted Values of Different Models in Terms of Depth, Full-Depth Asphalt Pavement: (a) Early Morning, (b) Noon, and (c) Evening; and Composite Pavement: (d) Early Morning, (e) Noon, and (f) Evening.

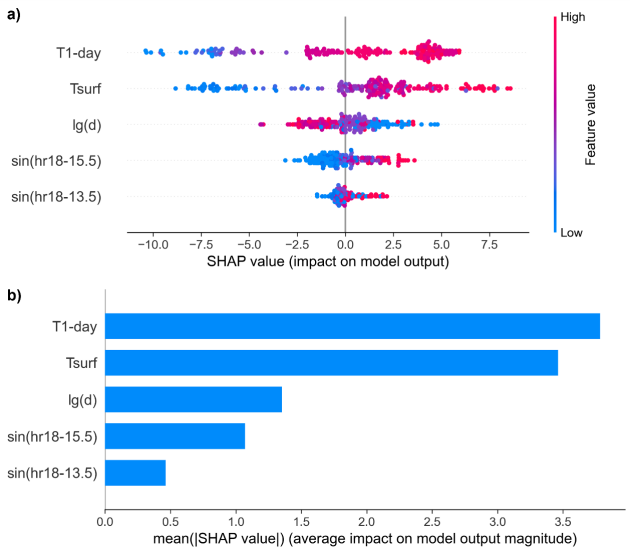

Figure 4.10 Feature Importance Analysis Results: (a) SHAP Values for Each Model Output, (b) Mean Value of Absolute SHAP Values.

surface temperature, which inherently reflects diurnal variation. The asphalt layer depth, expressed as *lg(d)*, showed a moderate influence on predictions, consistent with its role in defining the vertical temperature gradient.

4.8 Summary

This chapter investigated the potential of ML techniques to improve the prediction of pavement temperature gradients in full-depth asphalt and composite pavements. Key findings from the chapter are:

- Field data confirmed that surface temperature responds more rapidly and exhibits greater variation in response to environmental changes than internal pavement temperatures. As depth increases, temperature fluctuations diminish, with negligible variation observed beyond approximately 420 mm (16.5 in.).
- Among the four baseline empirical models, the original BELLS3 model provided the most accurate predictions before calibration, while the calibrated Idaho model outperformed the others after adjustment. However, ML models consistently achieved higher prediction accuracy. Even the simplest ML model—MLR—showed improvements over the empirical models. XGBoost demonstrated the best overall performance in terms of predictive accuracy.
- SHAP analysis of the XGBoost model revealed that the most influential variables were the "average air temperature of the day before testing" and the "pavement surface temperature." The time-of-day variables contributed less to the model's predictions, likely because their influence was already reflected in the surface temperature input.
- In conclusion, ML models, particularly XGBoost, offer an accurate and practical approach for predicting pavement temperature gradients using minimal input data. These findings support using

ML-enhanced models to improve temperature correction procedures for FWD and traffic speed deflectometer (TSD) deflections in flexible pavement analysis.

5. EFFECT OF PAVEMENT STRUCTURAL PARAMETERS ON TEMPERATURE SENSITIVITY OF FWD DEFLECTIONS

5.1 Introduction

The mechanical response of asphalt pavements is highly temperature-dependent, affecting FWD deflection measurements and, consequently, structural evaluations (Ai et al., 2018; D.-Y. Park et al., 2001). While field studies have explored these effects through repeated FWD testing at multiple times during the day (assuming constant structural capacity) or across different seasons to capture how deflections vary with temperature, they are limited by natural temperature variability and cannot always capture extreme conditions (W. Wang et al., 2018; Zheng et al., 2019).

To address this, FE modeling has emerged as a powerful alternative (B. Li et al., 2024). Calibrated FE models can simulate the viscoelastic response of asphalt pavements under different thermal conditions, allowing for the generation of controlled datasets of FWD deflections (B. Park et al., 2022; B. Park, Cho, Nantung, et al., 2023). Despite this advantage, many previous studies oversimplified the temperature distribution within asphalt layers, assuming uniform profiles or relying on empirical models such as BELLS3, which have been shown to yield inaccuracies in certain scenarios (Pais et al., 2020).

This chapter addresses that gap by integrating field-measured FWD data with FE simulations using realistic temperature gradients predicted by the ML-based model introduced in Chapter 4. A parametric analysis is conducted to quantify the influence of asphalt thickness and subgrade modulus on deflection behavior under varying thermal conditions in full-depth asphalt pavements.

5.2 Asphalt Viscoelastic Characterization

Dynamic modulus tests were conducted on core specimens extracted from six Indiana pavement sections to determine the viscoelastic behavior of asphalt layers in full-depth pavements. Following the same approach explained in Chapter 3.3, specimens from each asphalt layer (surface, intermediate, and base) were tested at three temperatures—4, 20, and 40° C (39, 68, and 104° F)—and three frequencies (0.1, 1, and 10 Hz) following AASHTO TP 132-19. The resulting dynamic modulus data were used to construct master curves by shifting the frequency data to a reference temperature of 20° C (68° F) using a sigmoidal fitting function. Master curves for each asphalt layer from the six selected pavement sections were developed and are shown in Figure 5.1.

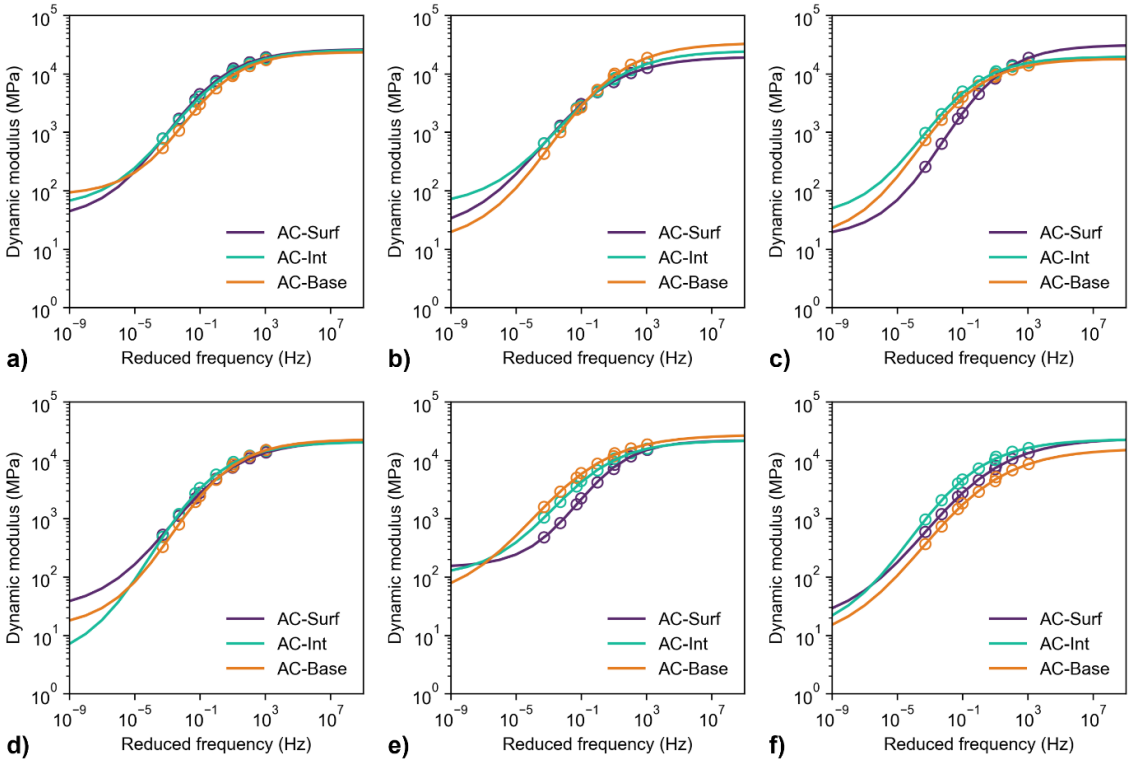

Figure 5.1 Fitted Master Curves of Different Asphalt Layers in Six Pavement Sections: (a) US 20, 9b) US 27, (c) US 31, (d) I-69, (e) SR 32, and (f) SR 545.

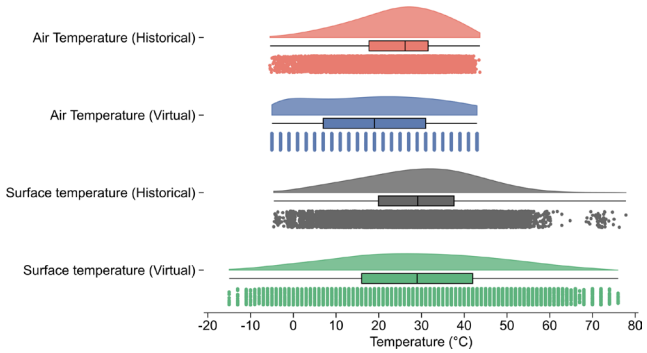

Figure 5.2 Comparison Between Virtually Model-Generated Temperature Data and Historical Actual Data.

As explained in Section 3.3.4, the master curves for each asphalt layer were then converted into relaxation modulus functions using a Prony series formulation, enabling their use as viscoelastic inputs in the FE simulations. To incorporate realistic thermal conditions into the FE modeling of pavement responses, temperature gradients across the asphalt layers were generated using a data-driven approach. The trained XGBoost model presented in Chapter 4 was used to virtually generate 1,150 temperature gradient profiles for each pavement structure by varying surface temperature inputs from -15° C (5° F) to 75° C (167° F) in 2° C (3.6° F) increments, along with associated average air temperatures and testing times. Historical surface temperature and air temperature records from INDOT were referenced to validate the plausibility of the generated scenarios. The comparison in Figure 5.2 confirmed that the virtual data closely matched historical trends, supporting its use in subsequent numerical simulations.

5.3 Parametric FE Analysis

A parametric FE analysis was conducted to simulate pavement responses under FWD loading, accounting for both the viscoelastic behavior of asphalt materials and the presence of temperature gradients. Simplified FE assumptions—such as neglecting these temperature- and time-dependent characteristics—often lead to significant inaccuracies. Therefore, this analysis integrated temperature-dependent material properties derived from laboratory testing and field temperature measurements. An axisymmetric FE model, similar to that described in Section 3.3.2, was developed and calibrated in Abaqus, which is particularly well-suited for simulating circular FWD loading due to its radial symmetry and computational efficiency compared to full 3D models (B. Park et al., 2022; B. Park, Cho, Nantung, et al., 2023; B. Park, Cho, Rahbar-Rastegar, et al., 2023).

A half-sine load with a frequency of 30 Hz and a peak pressure of 550 kPa (80 psi) was applied over a 300 mm (12 in.) diameter circular plate to simulate the FWD load. Model outputs were extracted at the peak load to capture the viscoelastic response of the asphalt layers under time-dependent loading conditions representative of actual FWD testing.

TABLE 5.1
Pavement Structures of Six Selected Sections.

Pavement section	Asphalt layer thickness (mm)				Subgrade modulus (MPa)
	Surface	Intermediate	Base	Total	
US 20	38.1	63.5	203.2	305	165
US 27	38.1	63.5	304.8	407	150
US 31	38.1	63.5	457.2	559	400
I-69	38.1	63.5	254	356	450
SR 32	38.1	63.5	355.6	457	150
SR 545	38.1	63.5	203.2	305	200

Six typical full-depth asphalt pavement sections from Indiana were used to define the geometric and material configuration of the FE models (Table 5.1). Each section included a surface, intermediate, and base asphalt layer, underlain by a subgrade. The subgrade modulus (M_r) for each section was backcalculated using the AASHTO 1993 Guide based on FWD deflection data, employing the following relationship:

$$M_r = \frac{0.24P}{d_r r} \tag{5.1}$$

where P is the applied load, d_r is the deflection at a radial distance r from the load center. It is noted that the deflection used to backcalculate the subgrade resilient modulus must be measured far enough away from the load center to provide a good estimate.

5.4 Surface Deflection Basins

The simulated FWD surface deflections under a wide range of pavement temperature scenarios revealed the substantial impact of temperature on pavement stiffness and structural response. Figure 5.3 presents the deflection basin profiles simulated across six representative pavement structures under a wide range of temperature scenarios. Each subfigure includes 1,150 FWD deflection basin curves, representing the vertical displacements at various radial distances from the loading center, capturing the viscoelastic response of the pavement system across temperatures ranging from -15° C to 75° C (5° F to 167° F). The color gradient from blue (cold conditions) to red (warm conditions) visually conveys the magnitude of surface deflections. As expected, higher pavement temperatures result in larger deflections due to the temperature-induced reduction in stiffness, while lower temperatures correspond to smaller deflections and stiffer pavement responses. Each case includes the specific pavement section details, notably the total asphalt thickness (T_{ac}, ranging from 305 mm to 559 mm, or 12 in. to 22 in.) and the subgrade resilient modulus (M_r, ranging from 150 MPa to 450 MPa, or 22 ksi to 65 ksi).

At low temperatures, deflection curves across all sections are relatively flat and concentrated, reflecting reduced viscoelastic deformation and high structural rigidity. In contrast, the spread and magnitude of deflection basins increase substantially at

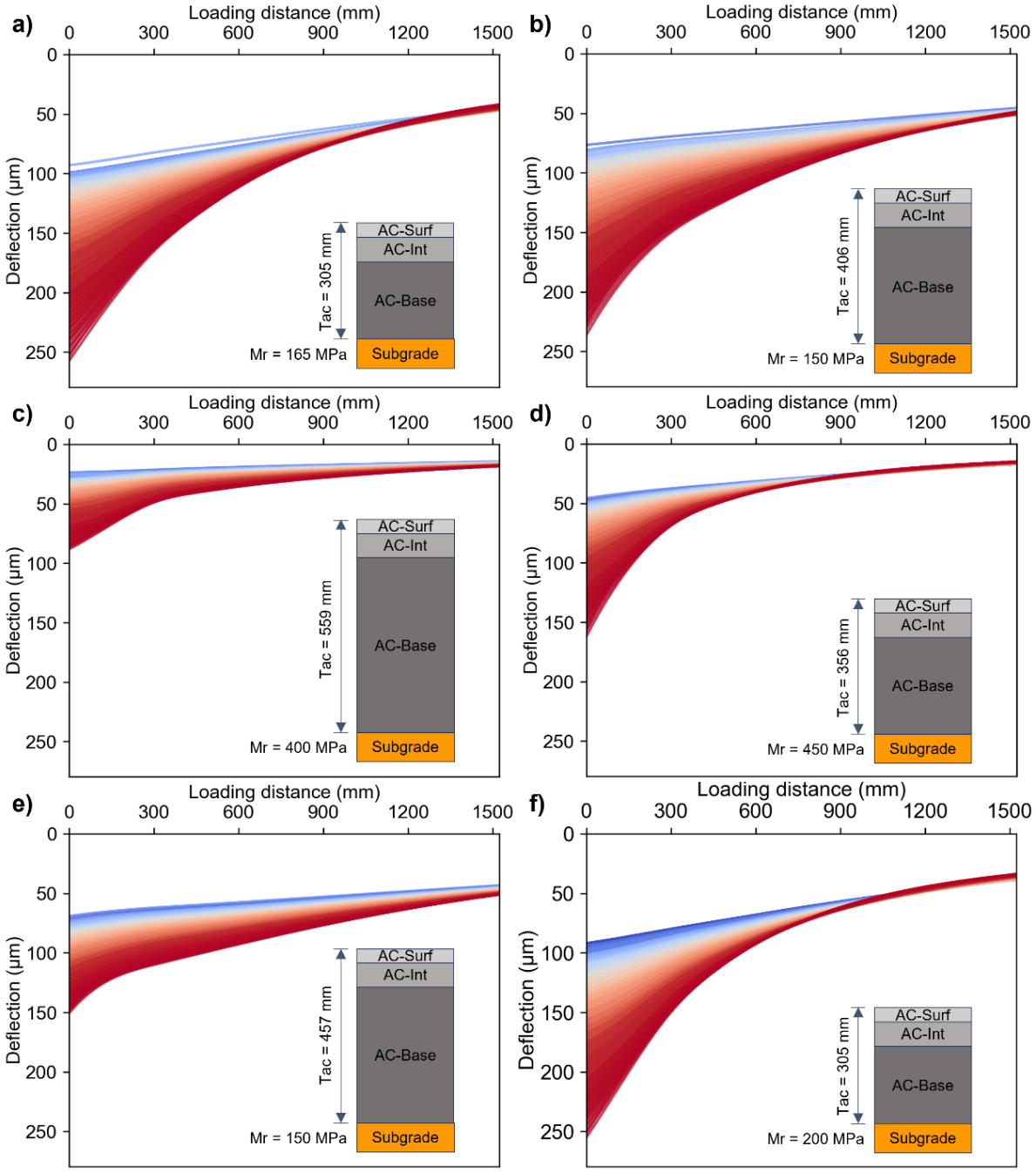

Figure 5.3 FWD Deflections Across Varying Pavement Temperature Scenarios, (a) US 20, (b) US 27, (c) US 31, (d) I-69, (e) SR 32, and (f) SR 545.

high temperatures, and structural differences become more evident. For instance, although US 20 and SR 545 have the same T_{ac} of 305 mm (12 in.), the lower M_r of US 20—165 MPa (24 ksi) compared to 200 MPa (29 ksi)—leads to more pronounced deflections. Similarly, US 31 exhibits lower deflections than I-69 despite comparable M_r values, attributable to its significantly thicker asphalt layer: 559 mm (22 in.) versus 356 mm (14 in.).

To further explore the thermal sensitivity of specific deflection metrics, Figure 5.4 plots deflections D0 and D1500 against the mid-depth temperature of the asphalt layers. Results show that D0 increases dramatically with rising temperature—up to 200% in some sections—whereas D1500 remains relatively constant. The sharp increase in D0, particularly above 50° C, highlights its sensitivity to asphalt softening, while the stable D1500 values indicate that temperature effects diminish with

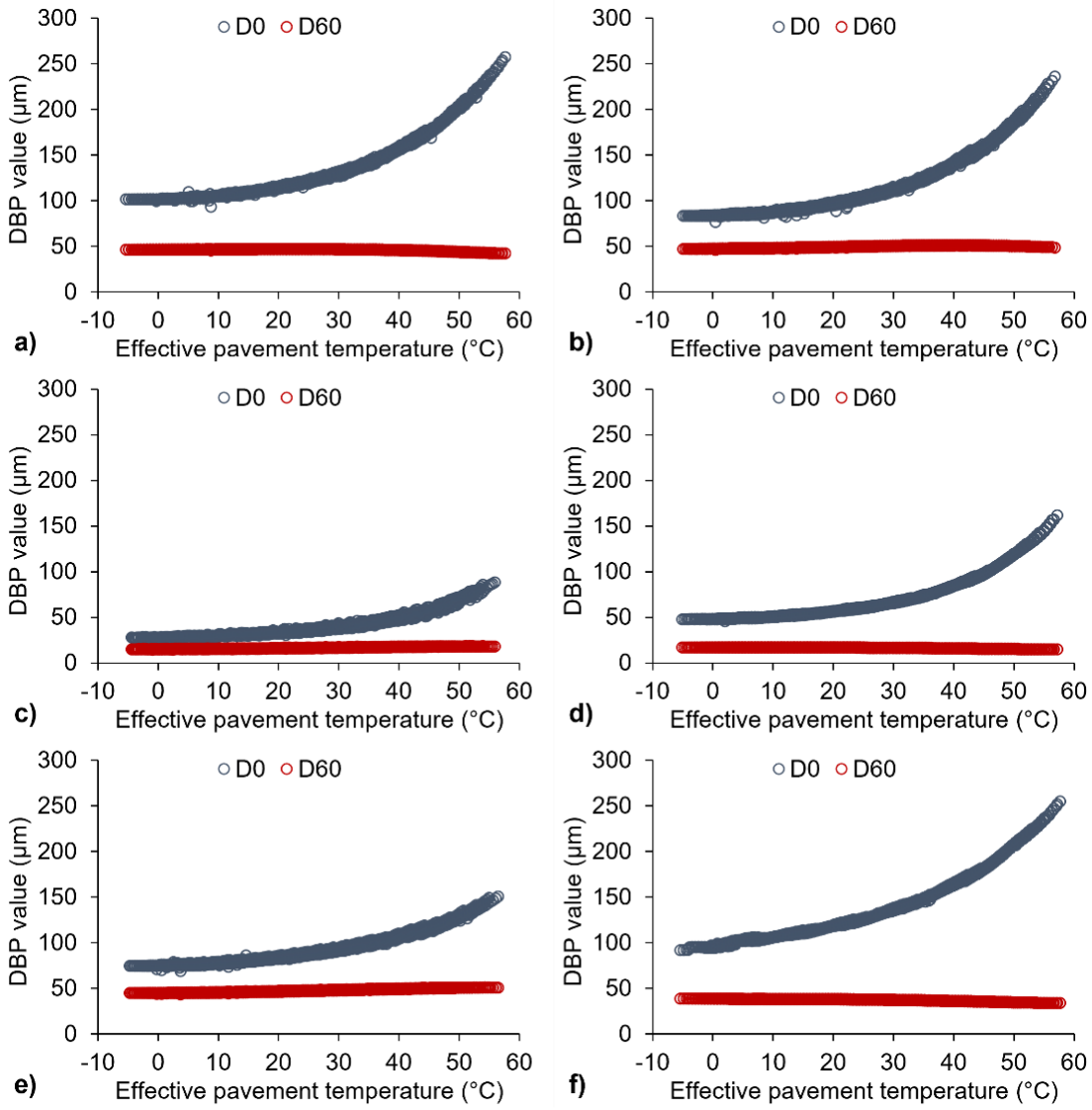

Figure 5.4 Central and Edge Deflections in Terms of Pavement Temperatures, (a) US 20, (b) US 27, (c) US 31, (d) I-69, (e) SR 32, and (f) SR 545.

radial distance from the load center. The trends are consistent across all pavement sections, although the rate and extent of change depend on structural factors such as T_{ac} and M_r.

For example, US 20 and SR 545, with lower M_r values, show greater D0 increases compared to sections such as US 31 or I-69, where stronger subgrade support mitigates temperature-related deformation. Moreover, thicker asphalt layers (e.g., in US 31 and SR 32) provide better insulation and distribute load-induced stresses more effectively, reducing the sensitivity of D0 to temperature changes.

To quantify the spatial extent of temperature influence on surface deflections, the coefficient of variation (CoV) was calculated for deflections at varying radial distances (Figure 5.5). The CoV, defined as the ratio of the standard deviation to the mean, decreases with distance from the FWD load center, indicating that the effect of temperature becomes less significant further from the load. Thresholds of 10% and 5% CoV were used to identify critical distances beyond which temperature variability is minimal. For instance, the 10% threshold yields effective distances ranging from 490 mm (19 in.) for I-69 to 1,000 mm (39 in.) for US 31, while the 5% threshold extends from 720 mm (28 in.) to beyond 1,500 mm (60 in).

These findings reveal that pavement structure plays a key role in the spatial extent of thermal effects. Sections with thinner asphalt or weaker subgrades (e.g., US 20 and US 27) display localized temperature influence with high CoV values near the center, indicating vulnerability to temperature-induced deformation. In contrast, sections with thicker asphalt and stronger subgrades (e.g., US 31, SR 32) exhibit more uniform temperature responses with broader zones of low variability. Intermediate trends were observed in sections with more balanced structural configurations (e.g., I-69, SR 545), suggesting moderate thermal sensitivity.

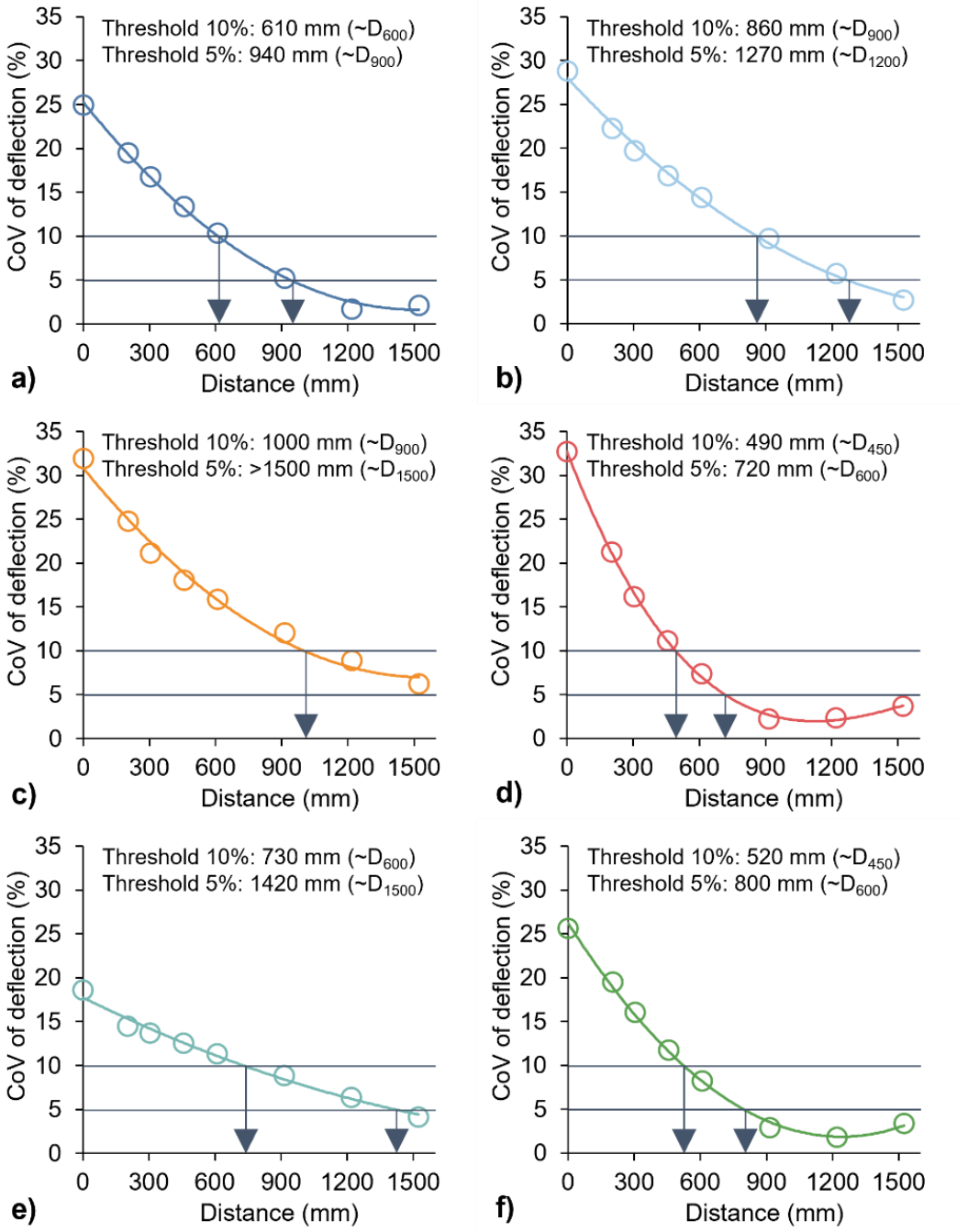

Figure 5.5 Temperature Effect Range (i.e., Effective Distance) of FWD Deflections, (a) US 20, (b) US 27, (c) US 31, (d) I-69, (e) SR 32, and (f) SR 545.

5.5 Contribution of Each Asphalt Layer

Figure 5.6 presents the relative contribution of individual pavement layers—namely, the asphalt surface (AC-Surf), intermediate (AC-Int), base (AC-Base) layers, and subgrade—to the total surface deflection under varying temperature conditions. The contribution of each layer was quantified by computing the deflection at the top of the layer and subtracting the deflection at the bottom (i.e., at the top of the underlying layer). These differences were then normalized by the total surface deflection to express each layer's share as a percentage of the overall response.

As expected, pavement temperature has a pronounced influence on the contribution of each layer. At low temperatures (around 0° C or 32° F), the subgrade dominates the structural response, contributing most of the surface deflection across all sections. However, as temperature increases—particularly

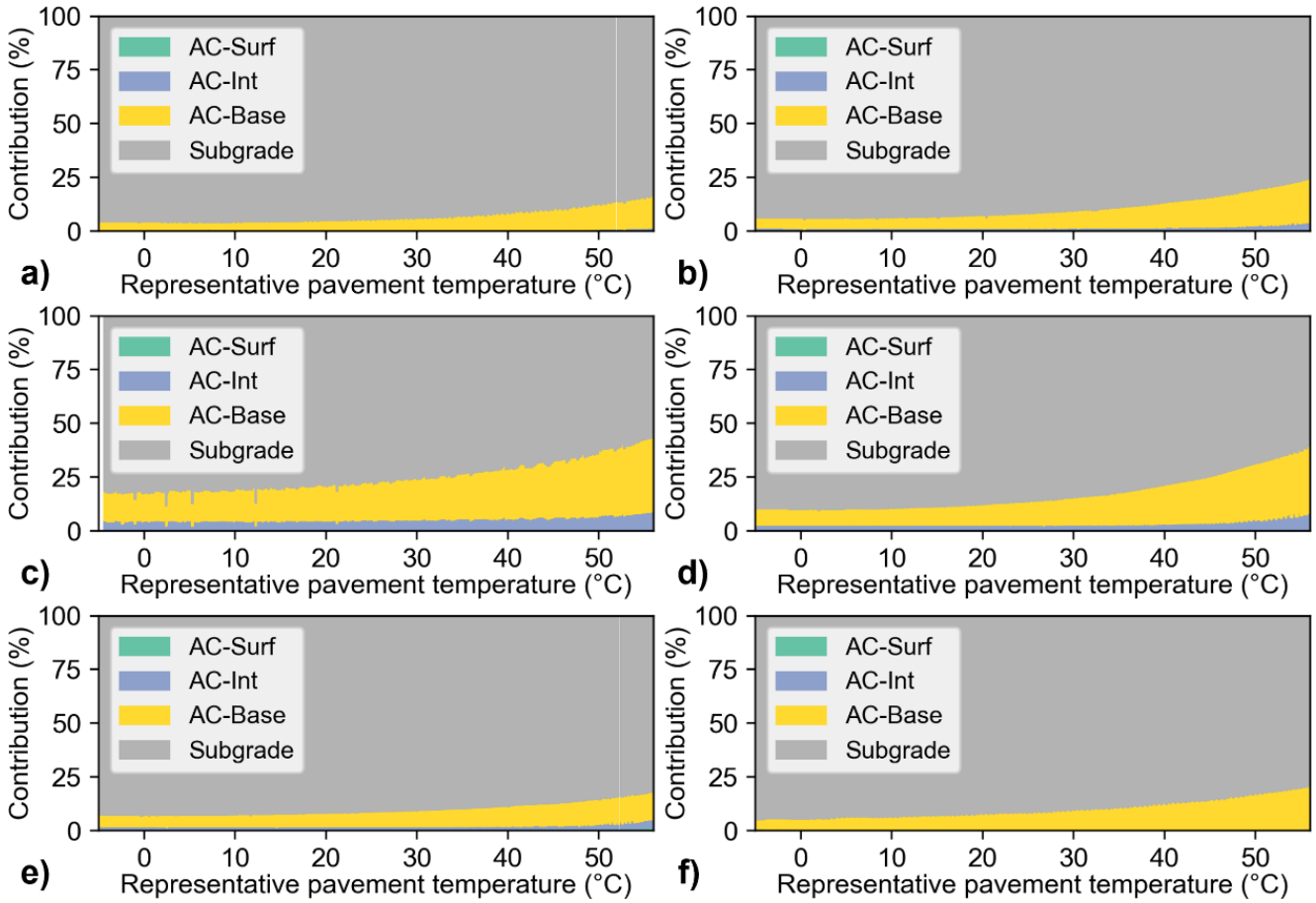

Figure 5.6 Contribution of Each Layer to Pavement Surface Deflections in Terms of Different Pavement Temperatures, (a) US 20, (b) US 27, (c) US 31, (d) I-69, (e) SR 32, and (f) SR 545.

beyond 30° C (86° F)—the stiffness of the asphalt layers decreases, causing their relative contribution to rise while the subgrade's role diminishes. Among the asphalt layers, the base layer shows the greatest sensitivity to temperature, especially in sections such as US 31 and I-69, where its contribution climbs to nearly 40% at high temperatures. This is likely due to its greater thickness and exposure to elevated temperatures compared to the surface and intermediate layers.

In contrast, the asphalt surface and intermediate layers generally contribute less, although their share also increases with temperature. In sections such as US 20 and SR 545, their influence remains minimal even under high-temperature scenarios, reinforcing the dominance of the asphalt base in temperature-induced deformation.

The structural configuration plays a key role in determining these trends. Sections with relatively thin asphalt layers and weak subgrades (e.g., US 20 and US 27) exhibit persistent subgrade dominance even at elevated temperatures, indicating greater reliance on subgrade support. Similar behavior is observed in SR 32, which, despite its thicker asphalt layers, has a relatively weak subgrade. In contrast, sections with both thick asphalt layers and stiff subgrades (e.g., US 31 and I-69) experience a pronounced shift in contribution: the asphalt base layer increasingly governs the structural response as temperatures rise, while the subgrade's influence quickly wanes.

These findings emphasize the need to consider the complete layer profile when analyzing deflection behavior under temperature variation, as well as the importance of asphalt base properties in high-temperature performance.

5.6 Summary

This chapter presented a comprehensive parametric FE analysis aimed at evaluating the temperature-dependent response of full-depth asphalt pavements under FWD loading. The simulations incorporated realistic temperature gradients, estimated using an enhanced prediction model, and accounted for temperature-sensitive viscoelastic properties of asphalt layers. The influence of structural characteristics—particularly asphalt layer thickness and subgrade modulus—was also examined. The key conclusions drawn from this study are as follows:

- **Influence of Structural Configuration**: Pavement structural features significantly affect the temperature sensitivity of

deflections. Thicker asphalt layers help attenuate surface temperature effects and distribute applied loads more effectively, resulting in reduced deflections. Similarly, higher subgrade modulus enhances overall structural support, mitigating deformation under thermal loads.

- **Spatial Extent of Temperature Influence**: Temperature-induced variability in FWD deflections diminishes with increasing distance from the load center. The effective influence range depends on the structural configuration: thinner asphalt layers and weaker subgrades result in shorter but more variable temperature influence zones, while thicker layers and stiffer subgrades yield broader and more uniform response patterns.
- **Layer-Specific Contributions to Deflections**: As pavement temperature increases, the contribution of asphalt layers to surface deflections rises, while that of the subgrade declines. Pavements with thicker asphalt sections and stronger subgrades transition more rapidly to asphalt-dominated responses, whereas those with thinner layers or weak subgrades remain governed by subgrade performance across temperature scenarios.

Overall, the results highlight the significant role of pavement structure in moderating temperature effects on FWD deflections. These findings can inform the development of refined temperature correction approaches for FWD measurements that consider structural parameters (such as asphalt thickness and subgrade stiffness) to enhance the reliability of pavement condition assessments under varying thermal environments.

6. DEVELOPMENT OF TEMPERATURE CORRECTION GUIDELINES FOR THE FWD DEFLECTIONS

6.1 Introduction

Accurate temperature correction of FWD data is essential to ensure reliable evaluation of pavement structural capacity, particularly in flexible pavements where asphalt layer stiffness is highly temperature-sensitive (Mehranfar & Modarres, 2020; Pais et al., 2020; Ramos García & Castro, 2011b). Although the AASHTO 1993 procedure remains the standard used by many highway agencies, it presents significant limitations—most notably, its restriction to correcting only the D0, limited applicability to asphalt thicknesses below 300 mm, and a vague definition of effective pavement temperature (D.-H. Chen et al., 2000; W. Wang et al., 2018). These shortcomings can lead to over- or underestimation of structural capacity, especially in thick flexible pavements such as full-depth asphalt pavements (Hermansson, 2002).

This chapter developed an enhanced temperature correction approach tailored to Indiana pavement conditions to overcome these shortcomings. The methodology is founded on the tools and approaches developed in previous chapters—namely, the XGBoost temperature prediction model (Chapter 4) and the viscoelastic FE simulations (Chapter 5)—which together form a robust and practical framework. The proposed correction factors account for deflections across all affected geophones (not just D0) and incorporate key structural parameters such as asphalt layer thickness, subgrade stiffness, and effective pavement temperature. Importantly, it eliminates the need for embedded temperature sensors by relying on predicted thermal profiles from easily obtainable inputs. The methodology was validated using field-collected FWD and temperature data, demonstrating improved accuracy and reliability over the AASHTO 1993 method for thick flexible pavements in Indiana.

6.2 Parametric FE Analysis

A comprehensive parametric study was conducted using FE modeling to assess the impact of temperature gradients and structural variability on FWD deflections. As detailed in Chapter 5, an axisymmetric FE model was developed and calibrated in Abaqus to simulate pavement behavior under FWD loading, incorporating the viscoelastic characteristics of asphalt materials. The model used a half-sine pressure pulse (30 Hz, 550 kPa peak pressure, 300 mm contact diameter) and captured responses at peak load, allowing accurate evaluation of time-dependent deflections.

Layer-specific viscoelastic properties were defined using a Prony series fitted to dynamic modulus data obtained from laboratory tests on field-extracted cores (see Chapter 5). These master curves were shifted to layer-specific mid-depth temperatures using time–temperature superposition, enabling the assignment of temperature-adjusted properties to each asphalt layer. Each layer was modeled with a uniform temperature, consistent with predicted gradients from the ML model developed in Chapter 4. This approach allowed for a realistic representation of thermal stratification with minimal computational overhead.

The FE model incorporated a range of pavement configurations by varying key structural parameters. Asphalt layer thickness ranged from 250 to 550 mm (10 to 22 in.), while subgrade modulus varied from 50 to 550 MPa (7 to 80 ksi), as detailed in Table 6.1. Together with temperature profiles spanning from -15° C to 75° C (59° F to 167° F), this modeling framework produced a robust dataset of synthetic FWD responses under a wide array of field-relevant conditions.

6.3 Determination of Temperature Correction Factors

To develop accurate temperature correction factors (C_T) for FWD deflections, this study first examined the central deflection, D0, which is most sensitive to asphalt temperature variations. As described in Equation (6.1), the C_T was defined as the ratio between deflection at a reference temperature (20° C or 68° F) and deflection at any given effective temperature, based on synthetic data generated via FE simulations. This allowed

TABLE 6.1
Pavement Structural Parameters.

Parameter	Values
Asphalt layer thickness (mm)	250, 300, 350, 400, 450, 500, 550
Subgrade modulus (MPa)	50, 100, 150, 200, 250, 350, 450, 550

consistent normalization of FWD measurements across a wide range of thermal conditions.

$$C_T = \frac{D_{ref}}{D} \tag{6.1}$$

where D_{ref} is the pavement surface deflections at the designated reference temperature and D is the pavement surface deflections at any given test temperature.

The analysis revealed a distinct sigmoidal relationship between effective pavement temperature (T_{eff}) and C_T (see Figure 6.1), which reflects the viscoelastic nature of asphalt materials. Asphalt layers exhibit high stiffness at low temperatures, resulting in smaller deflections and C_T values greater than 1. As temperature increases, asphalt softens, deflections increase, and C_T values fall below 1. This behavior closely mirrors the stiffness-temperature profile of asphalt mixtures, transitioning from a glassy to a rubbery state as temperatures

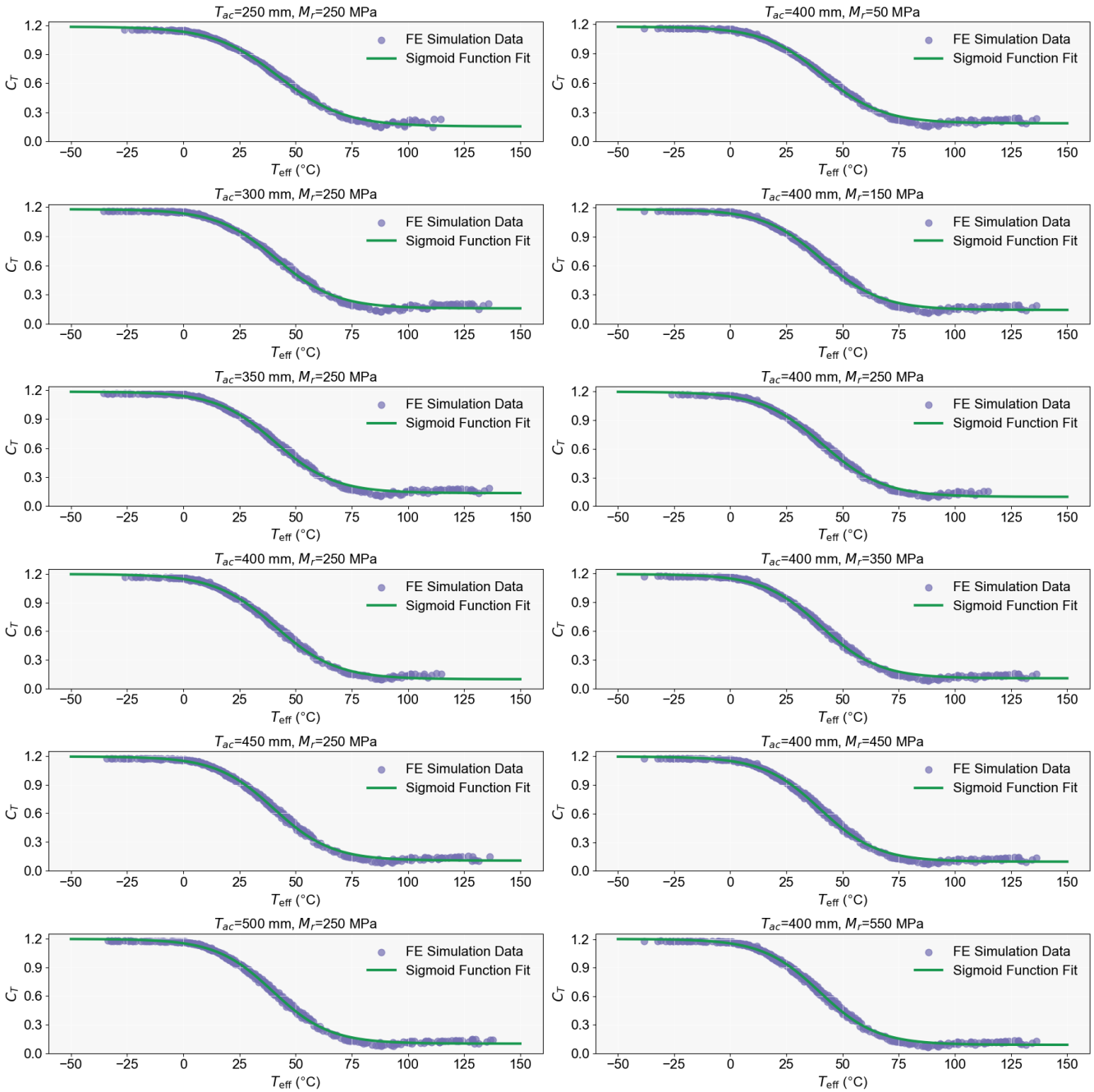

Figure 6.1 Relationship Between Effective Pavement Temperature and Temperature Correction Factors (C_T) for Varying Asphalt Thickness and Subgrade Modulus.

rise. At the reference temperature (20° C or 68° F), C_T equals 1 by definition.

To model this behavior, a modified sigmoid function was proposed:

$$C_T = \delta + \frac{\alpha}{1 + e^{\beta + \gamma \cdot T_{eff}}} \tag{6.2}$$

where δ, α, β, and γ are fitting parameters derived from the FE results. This equation provides a continuous and physically interpretable model for adjusting FWD deflections based on the T_{eff}.

As illustrated in Figure 6.2, further analysis demonstrated that pavement structural parameters significantly affect the magnitude and shape of the $C_T - T_{eff}$ curve. Two parameters, total asphalt thickness (T_{ac}) and subgrade resilient modulus (M_r), were systematically varied to assess their influence.

Asphalt thickness had a pronounced effect: thicker asphalt layers produced steeper C_T curves, with higher C_T values at low temperatures and lower C_T values at high temperatures. This indicates that thicker pavements exhibit greater sensitivity to temperature due to the increased contribution of temperature-dependent asphalt layers to total surface deflection.

Similarly, subgrade stiffness influenced the C_T trend. Higher M_r values led to greater C_T variation across the temperature range, as stiffer subgrades reduce subgrade deformation and amplify the temperature effects observed in the asphalt layers.

Together, these results confirm that temperature correction factors must be structure-specific. Generalized correction approaches—such as the AASHTO 1993 method—fail to capture the coupled influence of thermal gradients and structural configuration. The proposed methodology offers a more robust and accurate temperature correction framework for FWD analysis by explicitly incorporating asphalt thickness and subgrade stiffness.

6.4 Unification of Temperature Correction Functions

The relationship between C_T and T_{eff} consistently followed a sigmoidal pattern across all modeled pavement structures. However, the specific shape of each $C_T - T_{eff}$ curve was influenced by key structural parameters, T_{ac} and M_r. These structural dependencies affect the four fitting parameters (δ, α, β, and γ) of the sigmoid function used to represent C_T.

As shown in Figure 6.3, clear trends were observed between the sigmoid parameters (δ, α, β, and γ) and the pavement structural variables. To generalize the correction methodology, this study developed binary polynomial models to express each sigmoid parameter as a function of T_{ac} and M_r. For example, the parameter δ can be expressed as:

$$\delta = f_\delta(T_{ac}, M_r) = a \cdot T_{ac} + b \cdot M_r + c \cdot T_{ac}^2 + d \cdot M_r^2 + e \cdot T_{ac} \cdot M_r + f \tag{6.3}$$

where *a, b, c, d, e,* and *f* are dimensionless fitting coefficients.

Similarly, the other sigmoid parameters—α, β, and γ—are modeled using the same approach:

$$\alpha = f_\alpha(T_{ac}, M_r) = a \cdot T_{ac} + b \cdot M_r + c \cdot T_{ac}^2 + d \cdot M_r^2 + e \cdot T_{ac} \cdot M_r + f \tag{6.4}$$

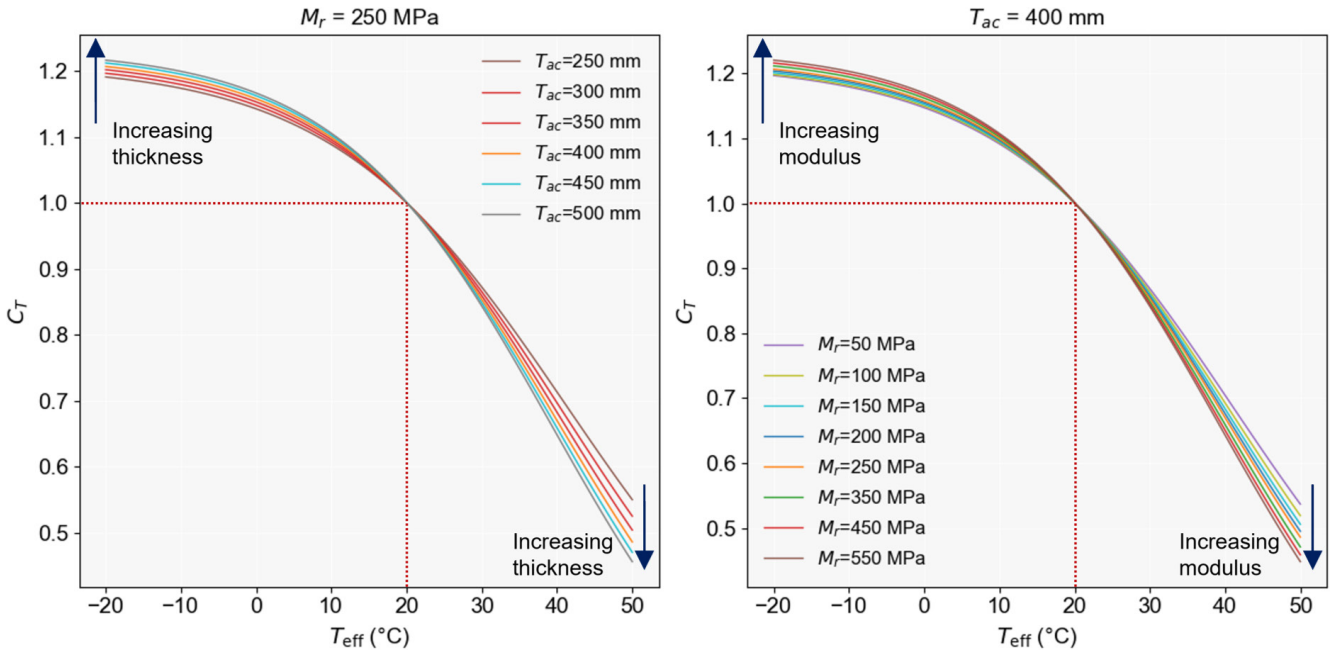

Figure 6.2 Influence of Asphalt Layer Thickness and Subgrade Stiffness on Temperature Correction Factors (C_T).

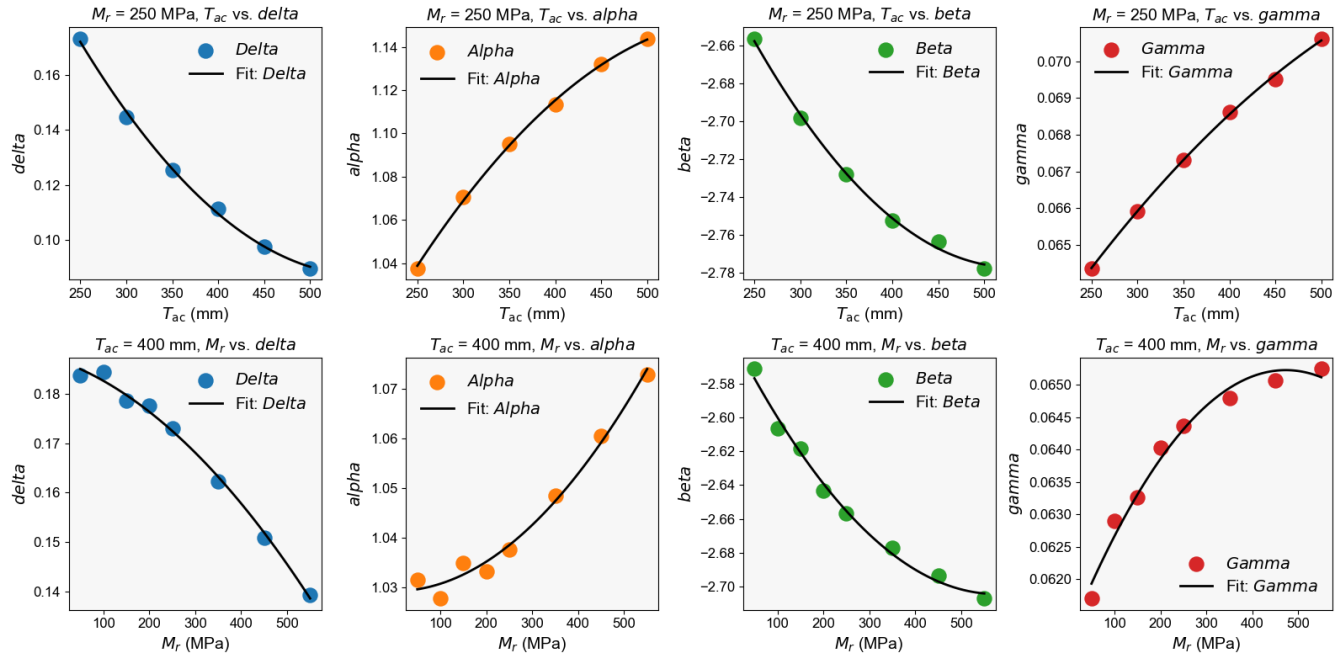

Figure 6.3 Correlation Between the Four Sigmoid Parameters and Two Pavement Structural Parameters.

$$\beta = f_\beta\left(T_{ac}, M_r\right) = a \cdot T_{ac} + b \cdot M_r + c \cdot T_{ac}^2 + d \cdot M_r^2 + e \cdot T_{ac} \cdot M_r + f \tag{6.5}$$

$$\gamma = f_\gamma\left(T_{ac}, M_r\right) = a \cdot T_{ac} + b \cdot M_r + c \cdot T_{ac}^2 + d \cdot M_r^2 + e \cdot T_{ac} \cdot M_r + f \tag{6.6}$$

These binary polynomial formulations enable a quantitative representation of how the sigmoid parameters vary with pavement structural characteristics. Figure 6.4 shows a strong agreement between the predicted and actual values of the sigmoid parameters, with R^2 exceeding 0.98 across all cases, indicating a highly accurate model fit. The corresponding dimensionless fitting coefficients (*a, b, c, d, e,* and *f*) for each parameter are provided in Table 6.2 for reference.

This approach allowed the development of a unified function for determining the C_T of pavement FWD deflections involving T_{eff}, T_{ac}, and M_r, which can be expressed in a modified form of the Sigmoid function as follows:

$$C_T = f_\delta\left(T_{ac}, M_r\right) + \frac{f_\alpha\left(T_{ac}, M_r\right)}{1 + e^{f_\beta\left(T_{ac}, M_r\right) + f_\gamma\left(T_{ac}, M_r\right) \cdot T_{eff}}} \tag{6.7}$$

While the proposed methodology primarily targets temperature correction of the D0, which remains the standard in current practice due to its high sensitivity to temperature, other deflections, such as D200, D300, and D450, also exhibit significant temperature-induced variability. To determine which deflections require correction, the CoV was evaluated for each across a range of pavement temperatures and structures, as shown in Figure 6.5.

As expected, CoVs generally decrease with distance from the load center; however, D0, D200, D300, and D450 consistently exceeded the 0.1 CoV threshold, suggesting that these deflections should also be temperature-corrected. Accordingly, the sigmoid function parameters for D200, D300, and D450 were determined using the same binary polynomial approach described earlier, with the resulting coefficients provided in Table 6.3, Table 6.4, and Table 6.5.

TABLE 6.2
Fitting Parameters of Binary Polynomial Functions for Each Sigmoid Parameter Based on Central Deflections, D0.

Sigmoid parameter	*a* (10^{-3})	*b* (10^{-6})	*c* (10^{-6})	*d* (10^{-6})	*e* (10^{-6})	*f*
δ	-20.32	-133.16	494.94	0.15	-6.11	0.36
α	20.78	49.66	-500.85	-0.13	13.39	0.85
β	-41.94	-783.61	912.21	0.65	13.39	-2.21
γ	1.08	14.59	-20.18	-0.02	0.53	0.05

TABLE 6.3
Fitting Parameters of Binary Polynomial Functions (for Deflection D200).

Sigmoid parameter	*a* (10^{-3})	*b* (10^{-6})	*c* (10^{-6})	*d* (10^{-6})	*e* (10^{-6})	*f*
δ	-29.35	994.10	849.59	-0.46	-35.37	0.49
α	31.91	-1220.26	-939.84	0.59	40.83	0.70
β	-45.64	-440.53	966.76	0.59	-17.84	-2.13
γ	0.55	37.23	-0.24	-0.03	-0.28	0.06

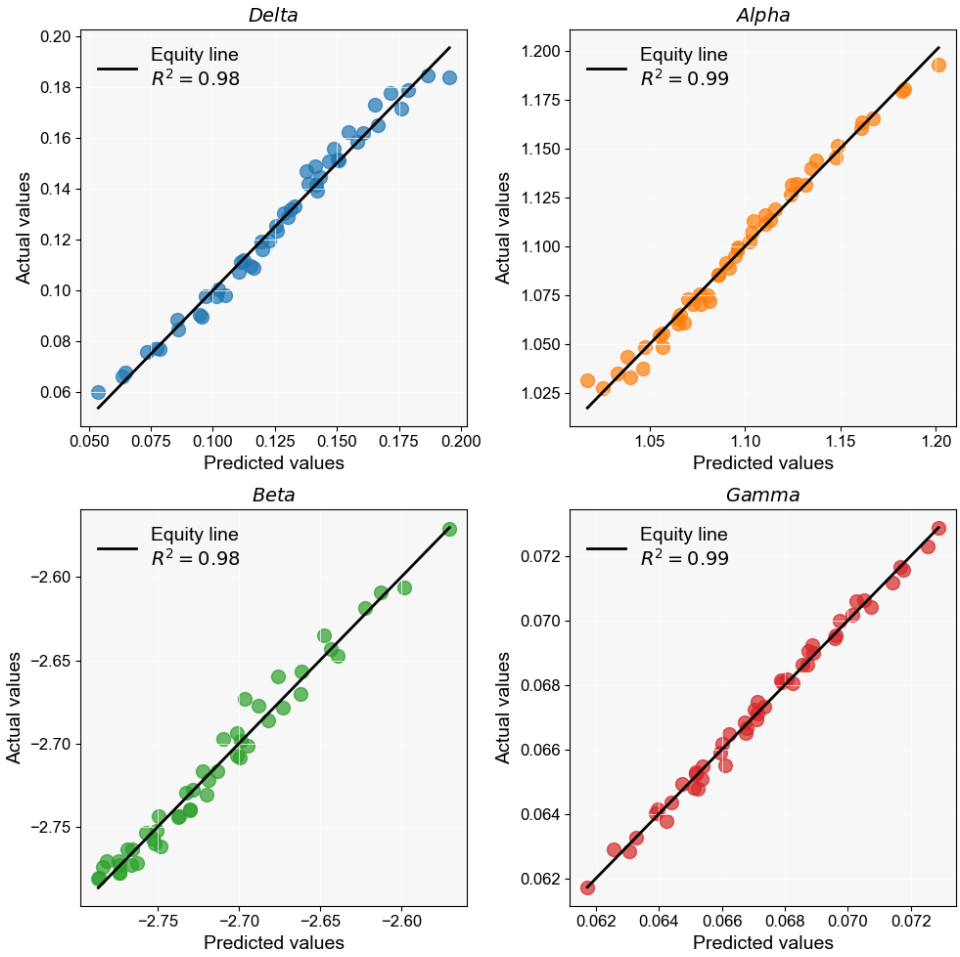

Figure 6.4 Agreement Between the Actual and Predicted Values of Sigmoid Parameters With High R^2 Values.

TABLE 6.4
Fitting Parameters of Binary Polynomial Functions (for Deflection D300).

Sigmoid parameter	a (10^{-3})	b (10^{-6})	c (10^{-6})	d (10^{-6})	e (10^{-6})	f
δ	-41.44	1508.66	1160.08	-0.70	-42.78	0.62
α	47.72	-1812.06	-1355.83	0.86	49.68	0.53
β	-40.39	-228.66	761.54	0.33	-14.45	-2.14
γ	-0.54	67.32	38.76	-0.02	-2.06	0.06

TABLE 6.5
Fitting Parameters of Binary Polynomial Functions (for Deflection D450).

Sigmoid parameter	a (10^{-3})	b (10^{-6})	c (10^{-6})	d (10^{-6})	e (10^{-6})	f
δ	-61.15	1846.71	1534.95	-1.07	-34.89	0.88
α	73.47	-2249.52	-1884.69	1.29	43.43	0.21
β	-17.71	-561.49	-200.81	-0.19	27.77	-2.22
γ	-4.22	146.49	165.34	-0.01	-6.37	0.09

6.5 Determination of Effective Pavement Temperature

While the AASHTO 1993 method offers a simple approach to correct FWD deflections for temperature, it lacks a clear definition of the T_{eff} to be used. Due to vertical temperature gradients in the pavement, selecting an appropriate T_{eff} remains a key challenge. Although many transportation agencies default to surface temperature—readily measured via FWD's infrared sensors—this may not accurately represent the thermal condition of thick, full-depth asphalt pavements (Orosa et al., 2025).

To address this, four T_{eff} candidates were evaluated based on literature and the characteristics of full-depth asphalt pavements with thick asphalt layers. These include:

- T_{mid}: mid-depth temperature of asphalt layers,
- T_{avg}: average of temperatures at 25 mm (1 in.) depth, mid-depth, and layer bottom (see Eq. (6.8)),
- T_{qua}: quarter-depth temperature, and
- T_{int}: temperature at the surface-intermediate interface.

$$T_{avg} = \frac{T_{25mm} + T_{mid} + T_{bot}}{3} \tag{6.8}$$

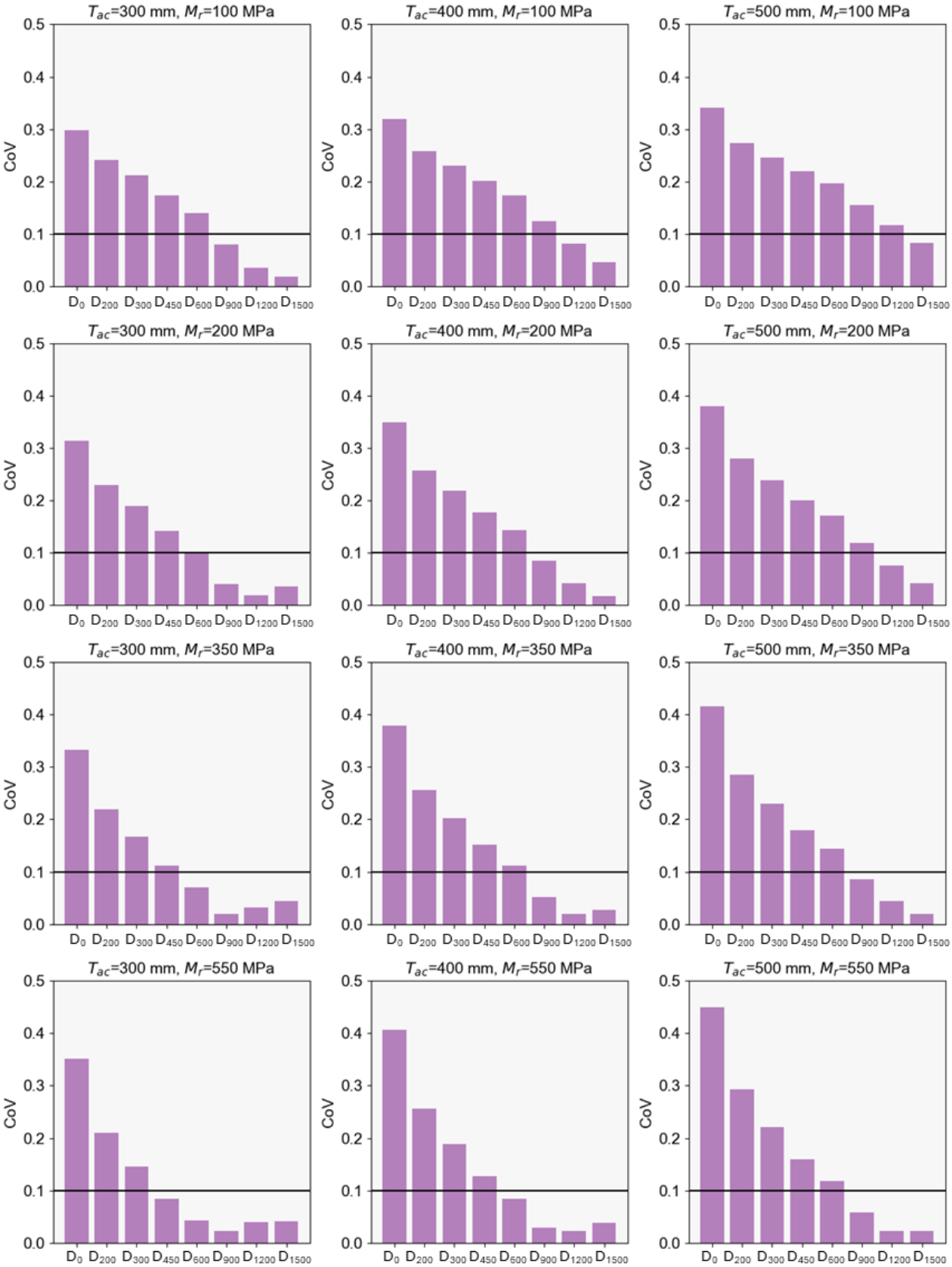

Figure 6.5 CoVs of Each FWD Deflection Across Varying Pavement Temperatures.

A new metric, referred to as Temperature Correction Difference Index (TCDI), was introduced to evaluate the effectiveness of each candidate. TCDI quantifies the consistency between corrected FWD deflection basins measured at two contrasting temperature scenarios (cool and warm). As illustrated in Figure 6.6, the corrected FWD deflection basins measured at different temperatures are supposed to be the same after temperature correction, and TCDI is thus defined as the accumulated percent difference between the two corrected FWD deflection basins. A lower TCDI value indicates better temperature correction performance.

Each T_{eff} candidate was assessed using field-collected deflection data and embedded temperature sensor readings from three instrumented full-depth asphalt sections. Figure 6.7 displays temperature profiles and corresponding FWD deflections, while Figure 6.8 summarizes TCDI results for each candidate.

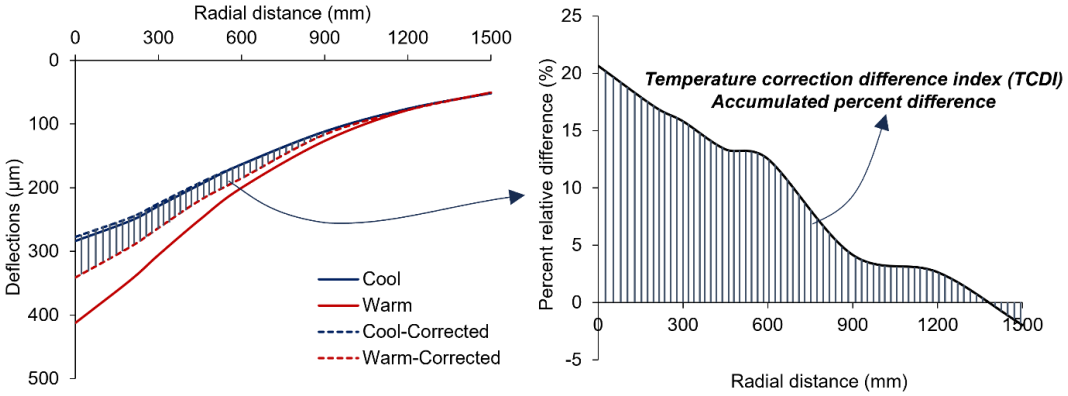

Figure 6.6 Illustration of TCDI.

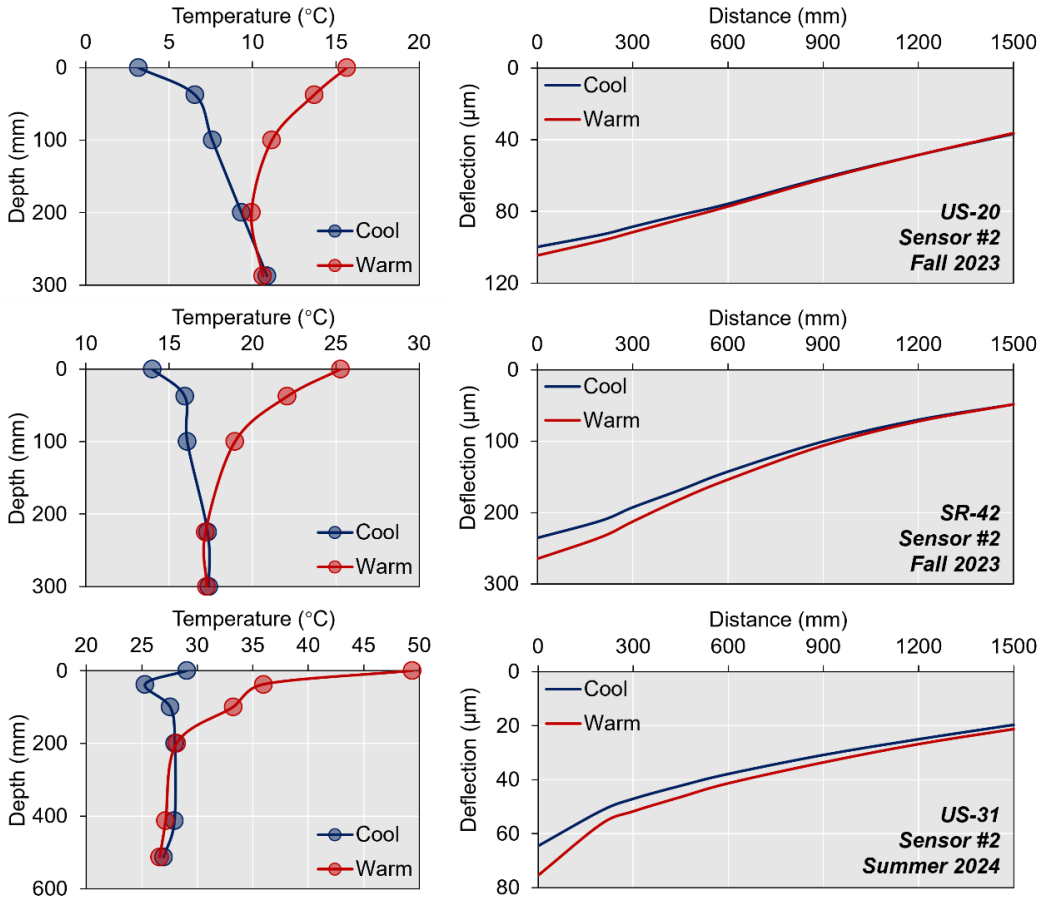

Figure 6.7 Field Temperatures and FWD Deflections Measured From Three Full-Depth Asphalt Pavement Sections.

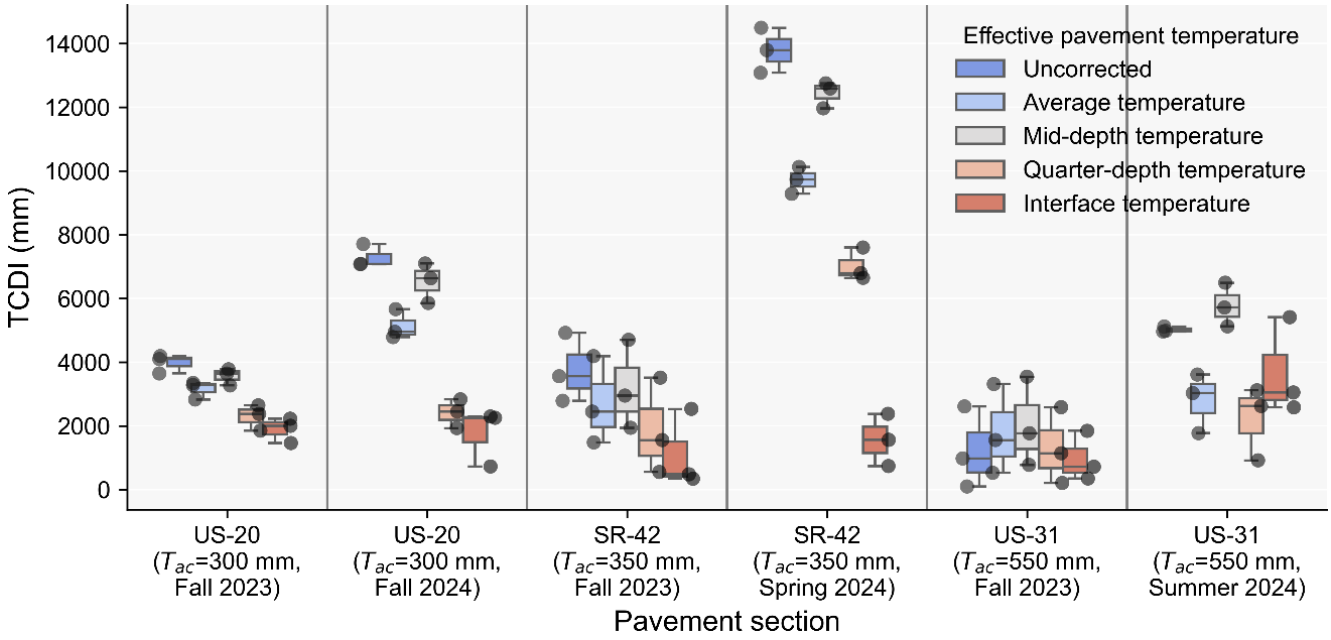

Figure 6.8 Effectiveness Comparison of T_{eff} Candidates.

The results reveal that T_{int} and T_{qua} consistently yield lower TCDI values, demonstrating superior performance in correcting for temperature. In contrast, T_{mid} and T_{avg}—often located beyond the daily thermal penetration depth (approx. 200 mm or 8 in.)—show minimal daily variation and are less responsive to surface temperature changes. Therefore, T_{mid} is not recommended for full-depth asphalt pavements.

For backcalculation of subgrade modulus in the analysis, the AASHTO 1993 expression described in Equation (5.1) was used.

These findings emphasize the importance of selecting a representative T_{eff} within the thermally active zone of the pavement, particularly for thick, full-depth asphalt pavement sections. T_{int} and T_{qua} offer a more accurate basis for calculating C_T and improving the reliability of temperature correction procedures.

6.6 Field Validation of Refined Methodology

After developing a unified temperature correction function and identifying suitable definitions of T_{eff}, this study proposes a new temperature correction methodology (NTCM) tailored for full-depth asphalt pavements. The NTCM was tested using field-collected FWD data across varying temperature conditions to validate its practical applicability and accuracy.

Field validation was conducted at six full-depth asphalt pavement sections in Indiana, selected to capture a wide range of temperature scenarios throughout the day. At each site, FWD deflections were measured during both cool and warm periods to assess temperature sensitivity. Instead of embedded sensors, temperature gradients were predicted using the ML model developed earlier (Chapter 4), enabling nonintrusive estimation of T_{eff} at different depths.

To assess the effectiveness of the proposed NTCM, its performance was compared against the conventional AASHTO 1993 temperature correction method (see **Error! Reference source not found.**). In accordance with common practice, the AASHTO method was implemented using either the mid-depth (T_{mid}) or the average temperature (T_{avg}) as the T_{eff}. For the NTCM, the two recommended T_{eff} candidates—T_{int} and T_{qua}—were used. Thus, five temperature correction strategies were compared:

1. No correction (uncorrected),
2. AASHTO 1993 using T_{mid},
3. AASHTO 1993 using T_{avg},
4. NTCM using T_{qua}, and
5. NTCM using T_{int}.

Each method's performance was quantified using the TCDI, which captures the cumulative percentage difference between corrected deflection basins from warm and cool conditions. Lower TCDI values indicate better correction accuracy.

Figure 6.9 presents the comparative TCDI results for all five correction methods. Results show that the NTCM significantly outperforms the AASHTO 1993 method across all sites, consistently producing lower TCDI values regardless of whether T_{qua} or T_{int} was used. This confirms the method's ability to effectively reduce temperature-related variability in FWD measurements.

In addition to improved accuracy, the NTCM is also practical for field use. It relies on machine learning predictions of pavement temperature using readily available data (e.g., ambient temperature, time of day, pavement thickness), eliminating the need for embedded sensors. This allows for estimating T_{eff} at meaningful depths, such as the surface-intermediate interface or

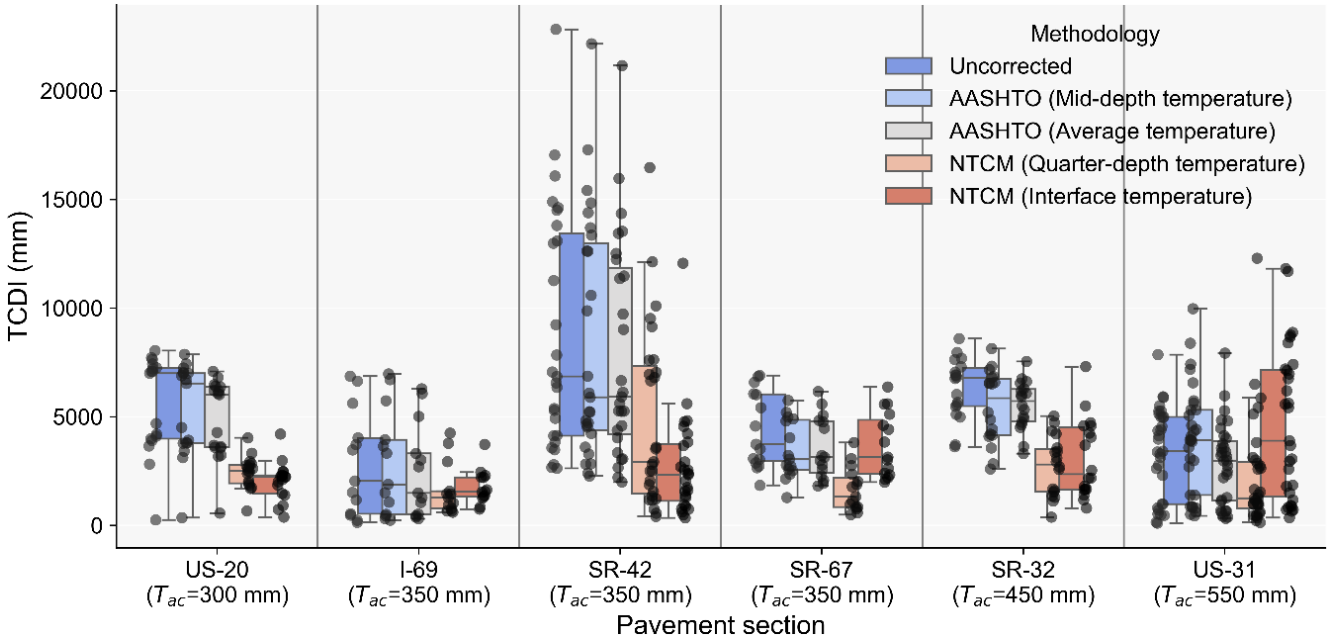

Figure 6.9 Field Validation of Proposed Temperature Correction Method and Comparison With AASHTO 1993.

quarter-depth, which are better suited for temperature correction in thick asphalt structures.

In summary, the NTCM provides a validated, data-driven, and field-ready methodology for temperature correction of FWD deflections in full-depth asphalt pavements. It potentially improves the accuracy of backcalculated moduli and supports more reliable pavement evaluation and design decisions.

6.7 Summary

This chapter comprehensively develops a new temperature correction methodology for FWD deflections in full-depth asphalt pavements. The proposed approach offers a more accurate, adaptable, and physically grounded framework for correcting temperature effects on pavement responses by integrating field temperature data, machine learning-based temperature prediction models, and viscoelastic FE analysis. The key findings are summarized below:

- **Accurate determination of temperature correction factors**: Parametric FE simulations covering a wide range of thermal conditions enabled the calculation of temperature correction factors (C_T). These were modeled using a unified sigmoid function, incorporating effective pavement temperature (T_{eff}), asphalt thickness (T_{ac}), and subgrade resilient modulus (M_r).
- **Correction across multiple deflection points**: Significant temperature sensitivity was observed not only in D0 but also in off-center responses such as D200, D300, and D450. This supports the need for correcting multiple FWD deflections—not just D0—for more accurate backcalculation.
- **Introduction of a performance metric**: A new metric, the TCDI, was introduced to evaluate the effectiveness of temperature corrections. It quantifies the consistency of corrected deflection basins across different temperature conditions.
- **Identification of suitable temperature measurement depths**: For full-depth asphalt pavements, internal temperature metrics such as the interface temperature (T_{int}) and quarter-depth temperature (T_{qua}) yielded better correction performance than mid-depth or average temperature values (T_{mid}, T_{avg}). This highlights the importance of accounting for limited thermal penetration in thick asphalt layers.
- **Superior performance of the new correction methodology**: The proposed NTCM—combining machine learning temperature predictions with a physically based correction model—consistently outperformed the conventional AASHTO 1993 method in field validation cases, offering improved accuracy and field implementation potential.

7. SUMMARY OF FINDINGS AND FUTURE WORKS

7.1 Findings

This report presents a comprehensive investigation into the effects of temperature on FWD deflections in flexible pavements, with special focus on full-depth asphalt pavements, and the development of an improved temperature correction methodology. The main findings are synthesized below:

7.1.1 Temperature Sensitivity of FWD Deflections

The field and FE-based FWD deflections analysis shows that deflections increase with rising pavement temperatures due to the viscoelastic nature of asphalt materials. However, the magnitude of this increase is not uniform. Pavements with thinner asphalt layers, lower subgrade stiffness, or deteriorated conditions exhibited larger temperature-induced variations. These effects extended beyond D0, affecting multiple sensors,

particularly under higher deflection levels. The traditional AASHTO 1993 method, which applies correction only to D0 based on surface temperature, was found to be insufficient, especially in structurally weaker sections.

7.1.2 Machine Learning for Pavement Temperature Prediction

ML models, particularly XGBoost, significantly outperformed empirical models in predicting pavement temperature profiles. These models used minimal and easily accessible inputs such as surface and previous day's air temperatures. The findings showed that while surface temperatures are highly variable, internal temperatures—especially beyond 400 mm (16 in.)—remain stable. This validates the use of ML-enhanced models as practical tools for estimating internal pavement temperatures without the need for embedded sensors.

7.1.3 Influence of Pavement Structural Parameters

The structure of the pavement, specifically asphalt thickness and subgrade modulus, plays a crucial role in moderating temperature effects on deflections. Thicker asphalt layers attenuate surface thermal fluctuations and distribute loads more effectively, reducing the temperature sensitivity of deflections. Similarly, stronger subgrades support stiffer responses. The spatial extent of temperature influence and the relative contribution of each layer to surface deflections vary with these structural parameters, emphasizing the need for correction methods that account for pavement configuration.

7.1.4 Development and Validation of a New Correction Methodology

A NTCM was developed by integrating results from viscoelastic FE simulations and ML temperature predictions. This approach models correction factors using a unified sigmoid function that depends only on effective pavement temperature (T_{eff}), asphalt thickness (T_{ac}), and subgrade resilient modulus (M_r). It enables correction across multiple deflection points and eliminates the need for embedded temperature sensors. Field validation confirmed that internal temperature metrics such as interface temperature (T_{int}) and quarter-depth temperature (T_{qua}) yielded more accurate corrections than mid-depth or average temperatures. The proposed method consistently outperformed the AASHTO 1993 procedure, improving accuracy and adaptability for full-depth asphalt pavements.

7.2 Future Work

While the proposed methodology represents a significant advancement, several areas of future research are recommended to further refine and expand its applicability:

- **Extension to Other Pavement Types**: Future work should investigate the application of this correction methodology to composite pavements and asphalt pavements with thinner layers or stabilized bases, where temperature gradients and structural responses may differ significantly.
- **Integration with Modulus Backcalculation**: While this study focused on deflection correction, subsequent work should explore the impact of the refined correction on backcalculated moduli. Evaluating the sensitivity of layer moduli to the new correction method could offer further insights for pavement design and rehabilitation.
- **Real-time Implementation**: Incorporating this methodology into field-operable tools and software for real-time temperature correction during FWD testing could greatly enhance its adoption. Integrating the machine learning model into agency workflows for automated T_{eff} estimation is a logical next step.
- **Broader Validation and Calibration**: Expanding the dataset used for training and validation, including diverse climatic zones, pavement structures, and materials, would further test the generalizability and robustness of the proposed approach.
- **Standardization and Agency Adoption**: Continued collaboration with transportation agencies could support the development of guidelines or standards that formalize the use of the NTCM as a supplement or replacement for legacy correction methods.

The framework developed in this study sets a foundation for more accurate, data-driven pavement evaluations and paves the way toward standardized temperature correction methods that reflect the true thermo-mechanical behavior of asphalt pavements.

REFERENCES

Abo-Hashema, M. A. (2013). Modeling pavement temperature prediction using artificial neural networks. In I. L. Al-Qadi & S. Murrell (Eds.), *Airfield and highway pavement 2013* (pp. 490–505). American Society of Civil Engineers. https://doi.org/10.1061/9780784413005.039

Adwan, I., Milad, A., Memon, Z. A., Widyatmoko, I., Ahmat Zanuri, N., Memon, N. A., & Yusoff, N. I. M. (2021). Asphalt pavement temperature prediction models: A review. *Applied Sciences*, *11*(9), 3794. https://doi.org/10.3390/app11093794

Ai, C., Rahman, A., Huang, D., Ren, D., & Lu, Y. (2018). Dynamic behavior and performance analysis of asphalt pavement in areas with extreme seasonal variation in temperature. *Journal of Transportation Engineering, Part B: Pavements*, *144*(3). https://doi.org/10.1061/JPEODX.0000063

Alavi, M. Z., Pouranian, M. R., & Hajj, E. Y. (2014). Prediction of asphalt pavement temperature profile with finite control volume method. *Transportation Research Record*, *2456*(1), 96–106. https://doi.org/10.3141/2456-10

Alawi, M. H., & Helal, M. M. (2012). Mathematical modelling for solving nonlinear heat diffusion problems of pavement spherical roads in Makkah. *International Journal of Pavement Engineering*, *13*(2), 137–151. https://doi.org/10.1080/10298436.2011.633166

American Association of State Highway and Transportation Officials. (1993). *AASHTO guide for design of pavement structures*. AASHTO.

Ayasrah, U. B., Tashman, L., AlOmari, A., & Asi, I. (2023). Development of a temperature prediction model for flexible pavement structures. *Case Studies in Construction Materials*, *18*, e01697. https://doi.org/10.1016/j.cscm.2022.e01697

Barber, E. S. (1957). Calculation of maximum pavement temperatures from weather reports. *Highway Research Board Bulletin, National Research Council*, *168*, 1–8.

Breiman, L. (2001). Random forests. *Machine Learning*, *45*(1), 5–32. https://doi.org/10.1023/A:1010933404324

Chen, D.-H., Bilyeu, J., Lin, H.-H., & Murphy, M. (2000). Temperature Correction on Falling Weight Deflectometer Measurements. *Transportation Research Record*, *1716*(1), 30–39. https://doi.org/10.3141/1716-04

Chen, J., Wang, H., Li, M., & Li, L. (2016). Evaluation of pavement responses and performance with thermal modified asphalt mixture. *Materials & Design*, *111*, 88–97. https://doi.org/10.1016/J.MATDES.2016.08.085

Chen, J., Wang, H., & Xie, P. (2019). Pavement temperature prediction: Theoretical models and critical affecting factors. *Applied Thermal Engineering*, *158*, 113755. https://doi.org/10.1016/J.APPLTHERMALENG.2019.113755

Chen, J., Wang, H., & Zhu, H. (2017). Analytical approach for evaluating temperature field of thermal modified asphalt pavement and urban heat island effect. *Applied Thermal Engineering*, *113*, 739–748. https://doi.org/10.1016/J.APPLTHERMALENG.2016.11.080

Chen, T., & Guestrin, C. (2016). XGBoost: A scalable tree boosting system. In *Proceedings of the 22nd ACM SIGKDD International Conference on Knowledge Discovery and Data Mining* (pp. 785–794). https://doi.org/10.1145/2939672.2939785

Cho, S., Park, B., Zhang, C., & Haddock, J. E. (2025). *Remaining service life prediction of Indiana pavements using mechanistic methods* (Joint Transportation Research Program Publication No. FHWA/IN/JTRP-2025/10). Purdue University. https://doi.org/10.5703/1288284317854

Dempsey, B. J., & Thompson, M. R. (1970). A heat transfer model for evaluating frost action and temperature related effects in multilayered pavement systems. *Highway Research Record*, *342*, 39–56.

Fernando, E. G., Liu, W., & Ryu, D. (2001). *Development of a procedure for temperature correction of backcalculated AC modulus* (Texas Transportation Institute Report No. FHWA/TX-02/1863-1). University of Texas at Austin. https://library.ctr.utexas.edu/hosted-pdfs/tti/1863-1.pdf

Gedafa, D. S., Hossain, M., & Romanoschi, S. A. (2013). Prediction of asphalt pavement temperature. In I. L. Al-Qadi & S. Murrell (Eds.), *Airfield and highway pavement 2013: Sustainable and efficient pavements* (pp. 373–382). https://doi.org/10.1061/9780784413005.029

Ghalandari, T., Shi, L., Sadeghi-Khanegah, F., Van den bergh, W., & Vuye, C. (2023). Utilizing artificial neural networks to predict the asphalt pavement profile temperature in western Europe. *Case Studies in Construction Materials*, *18*, e02130. https://doi.org/10.1016/j.cscm.2023.e02130

Han, D.-j., Li, C., Wei, X.-q., Yang, J.-l., Wu, C.-l., & Ouyang, Q. (2024). 2D temperature field analysis of asphalt pavements with three different types of subgrade structures. *Case Studies in Thermal Engineering*, *54*, 103964. https://doi.org/10.1016/J.CSITE.2023.103964

Hearst, M. A., Dumais, S. T., Osuna, E., Platt, J., & Scholkopf, B. (1998). Support vector machines. *IEEE Intelligent Systems and Their Applications*, *13*(4), 18–28. https://doi.org/10.1109/5254.708428

Hermansson, Å. (2002). Simulation of asphalt concrete (AC) pavement temperatures for use with FWD. *Road Materials and Pavement Design*, *3*(3), 281–297. https://doi.org/10.1080/14680629.2002.9689926

Hu, X., Li, J., Hu, Y., & Sun, L. (2022). Study on temperature correction of asphalt pavement deflection based on the deflection change rate. *Applied Sciences*, *13*(1), 367. https://doi.org/10.3390/app13010367

Huang, Y., Molavi Nojumi, M., Hashemian, L., & Bayat, A. (2024). Integrating machine learning for improved prediction of temperature and moisture in pavement granular layers. *Journal of Testing and Evaluation*, *52*(4), 2624–2642. https://doi.org/10.1520/JTE20230208

Huber, G. A. (1994). Weather database for the SUPERPAVE mix design system (Report No. SHRP-A-648A). Strategic Highway Research Program. https://onlinepubs.trb.org/onlinepubs/shrp/SHRP-A-648A.pdf

Hugo, F., Chen, D., Smit, A. D. F., Bilyeu, J., & River, R. (2001). Report on a comparison of the effectiveness of two pavement rehabilitation strategies on US 281 near Jacksboro (Center for Transportation Research Report No. FHWA/TX-0-1814-1). University of Texas at Austin. https://rosap.ntl.bts.gov/view/dot/14908/dot_14908_DS1.pdf

Inge, E. H., & Kim, Y. R. (1995). Prediction of effective asphalt layer temperature. *Transportation Research Record*, *1473*, 93–100.

Kassem, E., Bayomy, F. M. S., Williams, C., Saasita, E., Lamichane, S., & Permadi, D. D. (2020). *Development of pavement temperature prediction model* (Idaho Transportation Department Report No. FHWA-ID-20-279). Idaho Transportation Department. https://rosap.ntl.bts.gov/view/dot/56871/dot_56871_DS1.pdf

Ke, G., Meng, Q., Finley, T., Wang, T., Chen, W., Ma, W., Ye, Q., & Liu, T.-Y. (2017). LightGBM: A Highly Efficient Gradient Boosting Decision Tree. In I. Guyon, U. Von Luxburg, S. Bengio, H. Wallach, R. Fergus, S. Vishwanathan, & R. Garnett (Eds.), *Advances in neural information processing systems* (Vol. 30). Curran Associates, Inc. https://proceedings.neurips.cc/paper_files/paper/2017/file/6449f44a102fde848669bdd9eb6b76fa-Paper.pdf

Kim, Y. R., Hibbs, B. O., & Lee, Y. (1995). Temperature correction of deflections and backcalculated asphalt concrete moduli. *Transportation Research Record*, *1473*, 55–62.

Kim, Y. R., & Park, H. (2002). *Use of falling weight deflectometer multi-load data for pavement strength estimation* (North Carolina Department of Transportation Report No. FHWA/NC/2002-006). North Carolina State University. https://digital.ncdcr.gov/Documents/Detail/use-of-falling-weight-deflectometer-multi-load-data-for-pavement-strength-estimation/3709187

Li, B., Xie, Y., Bi, Y., Zou, X., Tian, F., & Cong, Z. (2024). Modeling and assessment of temperature and thermal stress field of asphalt pavement on the Tibetan Plateau. *Buildings*, *14*(7), 2196. https://doi.org/10.3390/buildings14072196

Li, J., Orosa Iglesias, P., Zhang, C., Moncada, O. A., Cho, S., Park, B., & Haddock, J. E. (2025). Enhanced temperature gradient prediction for asphalt layers in full-depth asphalt and composite pavement using machine learning techniques. *Transportation Research Record*, *2680*(3), 329–347. https://doi.org/10.1177/03611981251341325

Li, M., Wang, H., Xu, G., & Xie, P. (2017). Finite element modeling and parametric analysis of viscoelastic and nonlinear pavement responses under dynamic FWD loading. *Construction and Building Materials*, *141*, 23–35. https://doi.org/10.1016/j.conbuildmat.2017.02.096

Li, Y., Liu, L., & Sun, L. (2018). Temperature predictions for asphalt pavement with thick asphalt layer. *Construction and Building Materials*, *160*, 802–809. https://doi.org/10.1016/j.conbuildmat.2017.12.145

Lukanen, E. O., Stubstad, R. N., & Briggs, R. (2000). *Temperature predictions and adjustment factors for asphalt pavement* (FHWA-RD-98-085). Federal Highway Administration. https://highways.dot.gov/media/7551

Mehranfar, V., & Modarres, A. (2020). Evaluating the recycled pavement performance and layer moduli at variable temperature by non-destructive tests. *International Journal of Pavement Engineering*, *21*(7), 817–829. https://doi.org/10.1080/10298436.2018.1511784

Noureldin, S., Zhu, K., Harris, D. A., & Li, S. (2005). Non-destructive estimation of pavement thickness, structural number and subgrade resilience along INDOT highways (Joint Transportation Research Program Publication No. FHWA/IN/JTRP-2004/35). Purdue University. https://doi.org/10.5703/1288284313281

Ntramah, S., Tutu, K. A., Tuffour, Y. A., Adams, C. A., & Adanu, E. K. (2023). Evaluation of selected empirical models for asphalt pavement temperature prediction in a tropical climate: the case of Ghana. *Sustainability*, *15*(22), 15846. https://doi.org/10.3390/su152215846

Orosa, P., Li, J., Zhang, C., Park, B., Cho, S., & Haddock, J. E. (2025). Effective pavement temperature determination for improved falling weight deflectometer deflection correction in full-depth asphalt pavements. *Frontiers of Structural and Civil Engineering*, *19*(10), 1593–1601. https://doi.org/10.1007/s11709-025-1232-1

Pais, J., Santos, C., Pereira, P., & Kaloush, K. (2020). The adjustment of pavement deflections due to temperature variations. *International Journal of Pavement Engineering*, *21*(13), 1585–1594. https://doi.org/10.1080/10298436.2018.1557334

Park, B., Cho, S., Nantung, T. E., & Haddock, J. E. (2023). Field validation of falling weight deflectometer deflection-based critical strain prediction models for full-depth asphalt pavements. *Transportation Research Record*, *2677*(10), 635–645. https://doi.org/10.1177/03611981231162594

Park, B., Cho, S., Rahbar-Rastegar, R., Nantung, T. E., & Haddock, J. E. (2022). Prediction of critical responses in full-depth asphalt pavements using the falling weight deflectometer deflection basin parameters. *Construction and Building Materials*, *318*, 126019. https://doi.org/10.1016/j.conbuildmat.2021.126019

Park, B., Cho, S., Rahbar-Rastegar, R., Nantung, T. E., & Haddock, J. E. (2023). Use of falling weight deflectometer data to determine the effective structural number of full-depth asphalt pavements for structural condition assessment. *Road Materials and Pavement Design*, *25*(2) 276–290. https://doi.org/10.1080/14680629.2023.2200843

Park, D.-Y., Buch, N., & Chatti, K. (2001). Effective layer temperature prediction model and temperature correction via falling weight deflectometer deflections. *Transportation Research Record*, *1764*(1), 97–111. https://doi.org/10.3141/1764-11

Pierce, L. M., Bruinsma, J. E., Smith, K. D., Wade, M. J., Chatti, K., & Vandenbossche, J. (2017). *Using falling weight deflectometer data with mechanistic-empirical design and analysis, Volume III : Guidelines for deflection testing, analysis, and interpretation* (FHWA-HRT-16-011). Federal Highway Administration. https://www.fhwa.dot.gov/publications/research/infrastructure/pavements/16011/

Ramos García, J. A., & Castro, M. (2011). Analysis of the temperature influence on flexible pavement deflection. *Construction and Building Materials*, *25*(8), 3530–3539. https://doi.org/10.1016/j.conbuildmat.2011.03.046

Strategic Highway Research Program. (1993). *SHRP procedure for temperature correction of maximum deflections*. National Research Council.

Straube, E., & Jansen, D. (2009). Temperature correction of falling weight deflectometer measurements. In Bearing capacity of roads, railways and airfields: Proceedings of the *8th International BCR2A'09 Conference* (pp. 789–798).

Wang, D. (2012). Analytical approach to predict temperature profile in a multilayered pavement system based on measured surface temperature data. *Journal of Transportation Engineering*, *138*(5), 674–679. https://doi.org/10.1061/(ASCE)TE.1943-5436.0000362

Wang, D. (2013). Prediction of asphalt pavement temperature profile during FWD testing: Simplified analytical solution with model validation based on LTPP data. *Journal of Transportation Engineering*, *139*(1), 109–113. https://doi.org/10.1061/(ASCE)TE.1943-5436.0000449

Wang, W., Qiu, S., Wang, S., Wang, P., & Zhang, J. (2018). Investigation of seasonal variations of Beijing pavement condition data using unevenly spaced dynamic panel data model. *International Journal of Pavement Engineering*, *19*(9), 851–856. https://doi.org/10.1080/10298436.2016.1213590

Xiao, M., Luo, R., & Yu, X. (2022). Assessment of asphalt pavement overall performance condition using functional indexes and FWD deflection basin parameters. *Construction and Building Materials*, *341*, 127872. https://doi.org/10.1016/j.conbuildmat.2022.127872

Xu, B., Dan, H. C., & Li, L. (2017). Temperature prediction model of asphalt pavement in cold regions based on an improved BP neural network. *Applied Thermal Engineering*, *120*, 568–580. https://doi.org/10.1016/J.APPLTHERMALENG.2017.04.024

Yang, S., Qi, B., Cao, Z., Zhang, S., Cheng, H., & Yang, R. (2020). Comparisons between asphalt pavement responses under vehicular loading and FWD loading. *Advances in Materials Science and Engineering*, *2020*, 5269652. https://doi.org/10.1155/2020/5269652

Zheng, Y., Cai, Y., & Zhang, Y. (2011). Study on temperature field of asphalt concrete pavement. In D.-H. Chen, J.-R. Chang, M. Zaman, C. Zhao, & Z. Yao (Eds.), *Emerging Technologies for material, design, rehabilitation, and inspection of roadway pavements* (pp. 266–273). American Society of Civil Engineers. https://doi.org/10.1061/47629(408)33

Zheng, Y., Zhang, P., & Liu, H. (2019). Correlation between pavement temperature and deflection basin form factors of asphalt pavement. *International Journal of Pavement Engineering*, *20*(8), 874–883. https://doi.org/https://doi.org/10.1080/10298436.2017.1356172

About the Joint Transportation Research Program (JTRP)

On March 11, 1937, the Indiana Legislature passed an act which authorized the Indiana State Highway Commission to cooperate with and assist Purdue University in developing the best methods of improving and maintaining the highways of the state and the respective counties thereof. That collaborative effort was called the Joint Highway Research Project (JHRP). In 1997 the collaborative venture was renamed as the Joint Transportation Research Program (JTRP) to reflect the state and national efforts to integrate the management and operation of various transportation modes.

The first studies of JHRP were concerned with Test Road No. 1—evaluation of the weathering characteristics of stabilized materials. After World War II, the JHRP program grew substantially and was regularly producing technical reports. Over 1,600 technical reports are now available, published as part of the JHRP and subsequently JTRP collaborative venture between Purdue University and what is now the Indiana Department of Transportation.

Free online access to all reports is provided through a unique collaboration between JTRP and Purdue Libraries. These are available at docs.lib.purdue.edu/jtrp/.

Further information about JTRP and its current research program is available at engineering.purdue.edu/JTRP.

About This Report

An open access version of this publication is available online. See the URL in the citation below.

Orosa Iglesias, P., Li, J., Park, B., Cho, S., & Haddock, J. E. (2026). *Assessment of temperature correction factors for falling weight deflectometer deflections* (Joint Transportation Research Program Publication No. FHWA/IN/JTRP-2026/01). West Lafayette, IN: Purdue University. https://doi.org/10.5703/1288284318609